We would like to thank both reviewers for their overall encouraging statements about our manuscript, and for their constructive suggestions on how to improve it. In the following, we detail how we have addressed their comments in the manuscript revision.

The revised manuscript has track changes enabled which should make it easier for the reviewers and editor to see where revisions have been made.

Reviewer one:

The paper is generally very difficult to read, and I would suggest the authors to make substantial editing to the manuscript. As CO2 increases and SOA increases are quite different subjects, it is understandable that the paper covers a lot of different aspects. But this also requires the authors to pay attention to the organization of the paper (see some of the specific comments).

The modeling part and the observation part should be better integrated. Although the authors argued that the paper provided an example to study different process in a consistent observational and modeling framework, I feel the paper needs further work to better integrate observations and modeling results (see also some of the specific comments).

We have separated in the results section the observation and modelling aspects of the papers because of the different time scales covered (present-day, one growing season, vs. century perspective of the modelling), and because of the differences in geographic domain (forest vs. Siberia as a whole). This separation we would like to keep. Still, we hope that in response to the reviewer's points below (as well as in response to reviewer #2) the revised text has now a better "flow".

Section 2: The descriptions and discussions in this section are generally too long. I would suggest to move some of these discussions into Section 3 &4 and combine them with discussions in these two sections.

Re-reading the methods section, the reviewer is perfectly correct in that some of the text would fit better to the results section. Accordingly, we moved part of the text and adopted it to fit into Section 3 and Section 4;for instance, lines 280-86, 410-37. We also shortened parts of the remaining text.

Line 158: the model is set up to test CO2-inhibition hypothesis. It is not clear to me how this is achieved.

We have revised the sentence to make clearer to the reader how this is done (lines 157-163).

Line 247: where does 1.9 come from? Also, from Section 3.1, from line 274 to line 283, the range of E from 1.9 to 9.6 is also discussed. I feel it is better to move some of the discussion in Section 3.1 to Section 2.

We have moved most of the text on E*, and related text on how it is implemented in the DGVM (lines 410-427) to the discussion section, as suggested by the reviewer (we leave some in the results section as it is necessary when showing the range of simulated total BVOC emissions for Siberia/Table 1). In the methods/aerosol modelling, we refer the reader to the results section (lines 250-252); the reviewer is correct that the value without this reference is confusing.

Line 252, CCN at 1%. 1% seems too large.

We have decided to focus discussion on CCN at 1.0% supersaturation, since it reflects the changes in Aitken mode concentrations and local changes in precursor emissions (added to lines 256-58). We have now included an additional figure (A3) in appendix to indicate changes in CCN(0.2%). (see also response to a query by reviewer no. 2, corresponding to CCN supersaturation)

Line 271: For the "larch" plant functional type, an emission potential of E=2.4. But it in 247, E=1.9?

The value of 2.4 is an "old" value in the paper by Guenther et al., who at that time could not draw on any measurements on larch. We have moved this aspect to the discussion section and hope this has become less confusing (lines 421-27). For the aerosol modelling we had adopted the conservative, low end of measured E* (lines 495-96).

Table 1: description texts: the range of E from 1.9 to 9.6, and then a weighted one 6.4. Which one is used?

(Now Table 2) This is described in the table caption (slightly revised, for more clarity), and in the subscripts to the values given in the table (Total_MT_{BNS}): Simulations for monoterpene emissions for the boreal needleleaf summergreen (BNS) plant functional type compared three cases (indicated as subscripts for Total_MT_{BNS}): using maximum (9.6 $\mu g_C\ g^{-1}\ h^{-1}$) and minimum (1.9 $\mu g_C\ g^{-1}\ h^{-1}$) values for E^* measured in Spasskaya Pad (see text), and $E^* = 6.2 \mu g_C\ g^{-1}\ h^{-1}$ as a weighted average from all observations at the Spasskaya Pad location.

Section 3: Observations and modeling results are not well integrated. For example, why not compare simulated aerosol concentrations with observed present aerosol concentrations? *….I would like to see how present day BVOC and aerosols are simulated compared with observations.*

We have added a comparison of present-day daily BVOC model results for the Spasskaya Pad location against observations, using site-specific data, and some examples from literature (lines 293-301), and also included a data-model comparison in lines 464-473.

Section 3.3: Is CO-inhibition implemented in the sensitivity tests? This is not clear to me from reading Section 3.3. But line 158 seems to suggest this was tested in the paper.

We added clarifying statements to the revised section 3.3 (lines 360, 376)

Section 4: How is CO2 forcing calculated?

The method of calculating CO-radiative forcing follows the widely applied, standard methodology used eg. in each of the IPCC reports; for simplicity we assume an ocean uptake of 50% such as done in Stich et al. (see references given in the methods, lines 211-12)

Line 399: the sensitivity of CCN to E. This is not clear to me.

We agree that this is confusing to the reader, and is indeed not really visible in the Figures we have chosen to show. We removed the sentence.

Lines 424-434: This paragraph needs further editing. For example, it is not clear why the authors want to discuss changes in wildfire emissions and anthropogenic SO2 emissions. Later, it seems that the effects of BVOC are only assessed by assuming wildfire and anthropogenic CO2 unchanged. Many more paragraphs have similar issues. This is why the paper is really hard to read.

The challenge of understanding changes in aerosol load arise from competing factors that can either lead to enhancing or lowering aerosol burden. The chief reason why we need to add the discussion on wildfire and SO2 arise from the fact that the background load and size distribution are important for whether or not the enhanced BVOC lead to enhanced SOA and CCN production or not. Wildfires, in particular, are an important feature of boreal forests. However, the reviewer is correct that the paragraph had been confusing – in fact, we had at some stage in the analysis attempted to look at changing wildfire emissions but then realized that this would make the manuscript very complex (w.r.t. to the SOA analysis) and distract from the main story of the paper. We have revised the paragraph and hope that this has now become easier to understand. Overall, we believe that (in response to the reviewer's suggestions) the revised manuscript has become easier to read (lines 505 onwards).

Technical corrections:

Line 29: miss "." Between "effect" and "Combining".

Thanks, well spotted.

Line 32-35: The sentence of "On the global level, . . ." needs some further work.

The sentence has been revised.

Line 97: Make sure the citation format is correct.

We couldn't find an error with the format, but will check again in the type-set version.

Line 102: "BVOCs e.g.," → *"BVOCs (e.g.,"* ?

Thanks, corrected.

Lines 120-123: What are the units of Q, CGR, CS?

The units for these variables have now been added to the revised manuscript (lines 121-124 & Figure caption Figure 2).

Line 213: "components black carbon" → "components of black carbon"

Sentence has been revised.

Reviewer two:

I would suggest the authors to improve the readability of the manuscript through more diagrams and tables: - A schematic diagram summarizing the investigated interaction mechanisms; - A table with details of model configuration and highlighted new/important parameterization/treatment; - A table summarizing uncertain processes or those not sufficiently considered.

In response to this suggestion we have included in the methods section a new table 1, which summarises some of the critical model features. We contemplated also, as suggested, a table that summarises the missing processes, but felt in the end that this would not add crucial new knowledge, and keep this in the text at the end of the conclusion section.

Page 27142 line 24, "Aerosol particles were continuously monitored with a Scanning mobility particle sizer (SMPS) located at the foot of the eddy covariance tower ... ", how about the inlet system for aerosol measurements, were the aerosols sampled also from 30 m above the ground? If not, a difference between above and below canopy will be expected challenging the results of Fig. 2. To test the difference, I would suggest the authors to make similar comparison (as Fig. 2) but for a single species below and above the canopy, e.g., monoterpene (or other VOCs, trace gases).

A comparison of below and above canopy measurements is unfortunately not possible since neither for the BVOC nor for the aerosol concentration measurements along canopy vertical profile was possible in this extremely remote location. However, the way the aerosol sampling was conducted is similar to the well-established methodology applied in many aerosol monitoring locations (Nieminen et al., 2014). Since aerosols are monitored regarding the change in number and size distribution (not their flux) and the typical life-time of particles in the studied size range is close to a day or more, there is no difference expected between an inlet below or above the canopy. Among others, e.g. Nieminen et al., 2014 have shown that nucleation events are regional phenomena that can be measured at the same time within the space of several hundreds of square km.

Page 27142 line 24, please define the acronym "DGVM"

Thanks for spotting this, is now defined in line 127.

Page 27144 line 4, "A recent data-base estimate was 191, 495, and 1024 GtC in the 0–30, 0–100 and 0–300cm soil layer, of permafrost-affected soils, respectively". Are these estimates from observations or from models? What is the geographical coverage of these values (Eastern Siberia or above 40 degree N)?

The data are extrapolated from observations and are for high latitude soils affected by permafrost globally (ie, not including permafrost soils in mountains). The sentence is revised for clarification (now in lines 274-276).

Page 27145 line 1, " Multiple interacting processes can thus lead to enhanced global monoterpene emissions in future, or -if the "CO2 inhibition" is included- yield emissions that are more or less similar to present-day or even slightly smaller ". Can you elaborate how the CO2 inhibition was parameterized in your model?

We have added a short explanation to the methods text, see also response to reviewer one.

Page 27148 line 11, "The assumption of unchanging oxidant fields induces some uncertainty . . . The model climate is nudged towards ERA-40 reanalysis year 2000 meteorology, an approach that is widely used in aerosol-climate assessments". Did you use the same oxidative capacity field and nudging meteorology field for the year 2000 and 2100?

The oxidant fields and nudging meteorology are same for both 2000 and 2100. This allows us to study the sensitivity of CCN to BVOC emissions while assuming no changes in oxidative capacity or general circulation. We made this point more obvious, and moved it to the discussion section (see also response to request by reviewer one), lines 486-492.

Such treatment is OK for a sensitivity study but I am not sure if it is appropriate when you draw conclusions for a specific year 2100. Changes of land uses and VOCs will change the distribution of oxidants and meteorology.

The reviewer is correct in that we should be careful in some places for using a specific year for the ECHAM SOA and radiative effects.– which in fact wasn't really intended, even though we probably used "2100" in a too simplified way. In some cases this was correct, especially when referring to BVOC emissions that were input to the SOA simulations since these were indeed taken from a specific year from LPJ-GUESS transient 20th-21st century simulation. But in other cases we have revised the text, indicating that we mean to simulate conditions towards the end of the 21st century.

Page 27148 line 27, the authors used 1% supersaturation CCN. The atmospheric relevance of supersaturation depends on the aerosol concentration and updraft velocity. It will be better if the authors could give CCN at multiple supersaturations (e.g., in the supplement).

Page 27155 line 15, " What is more, SOA formation only partly enhances the survival of small particles by providing additional growth (Makkonen et al., 2012a), but partly also suppresses it by increasing the coagulation sink for small particles (Fig. A2, lower left panel; see also O'Donnell et al.,2011)".

CCN is defined for a specific supersaturation. Larger particles are better CCN (activated at lower supersaturation) than smaller ones. Though the coagulation removes smaller particles reducing the CCN number concentrations at high supersaturation, it increases the particle size leading to more good CCNs (activated at lower supersaturation). This is another mechanism affecting the indirect radiative effect of aerosols.

The manuscript uses CCN at 1.0% supersaturation to estimate potential effect on cloud properties. We agree that "realistic" supersaturations are generally lower than 1.0%, hence, CCN(1.0%) concentration as such provides the upper limit for CCN concentration. In the simulations, one must also bear in mind that in aerosol model M7, CCN(1.0%) might correspond to a cut-off diameter inside Aitken mode, whereas CCN(0.2%) cut-off is generally between Aitken and accumulation modes. CCN at 0.2% reflects larger aerosols, hence the changes in CCN(0.2%) likely seen further away from aerosol and precursor sources. We have included a new(CCN(0.2%)) figure in the appendix (Figure A3) corresponding to summer concentration changes averaged over 5 years. We also include explanatory text in lines 517-521.

Page 27150 Section 3.2, It is not clear for me how this section is linked to the modeling part of this study. Do you use it in the model parameterizations?

We have included the measurements to demonstrate that there are clear links between the concentrations of MT and SOA formation (e.g., Section heading and Figure 2). While this has been shown for a number of boreal forest sites we felt it important to also demonstrate this effect for Eastern Siberia, as an important basis for the model experimental set-up, because of its strong focus on BVOC emission effects on aerosol. We had also highlighted later in the text that an extrapolation of observation-based radiative forcing estimates to future forcings over large regions is not possible (lines 452-463). Data were not used for model parameterization in case of aerosol modelling.

Page 27151 line 14, "Hence, the poor relation between the source rate of condensing vapour and levels of radiation (Fig. 2b) indicates that OH-radical concentration did not have a major impact on Q. This agrees with the findings by Ehn et al. (2014) that ozone instead of OH. is an important, if not the main, atmospheric agent oxidizing organic vapours into a chemical form that condenses on particle surfaces."

I am not convinced by this argument because OH has a short life time and may have a large difference below and above the canopy, how about the correlation between Q and O3?

Hens et al. (2013) have shown that the OH concentrations below and above canopy are indeed quantitatively different, but have a clear correlation and variability thus agrees qualitatively. The strong variation in the OH concentrations, which can be more than an order of magnitude within the matter of hours around sunrise and sunset (e.g. Petäjä et al., 2009 and Hens et al., 2013), should have a clear impact on Q if OH was the dominant oxidant converting MT to condensable vapors. And since the OH concentration is strongly affected by radiation (also below the canopy; Petäjä et al., 2009), the impact of OH concentration on Q should also be visible in Fig. 2b.

Unfortunately, we could not inspect the correlation between Q and O3 (or Q and MT ozonolysis rate), because the remoteness of the site limited measurement capacity, and ambient ozone concentration measurements were not conducted during the campaign. However, even if we assumed that O3 is the only oxidizer affecting on Q, we

would not expect a clear correlation between Q and O3, because the relative variation in O3 concentrations is much smaller than that of monoterpenes (during the campaign by Hens et al. (2013), the variation of O3 concentration was within a factor of three, whereas the observed variation in MT concentrations reached factors of 10 to 100). The correlation we show in Fig. 2b suggests that Q is not heavily affected by the oxidant concentrations, which supports the assumption of O3 being the main oxidant. We have made further clarifications in the manuscript, regarding to OH concentrations above and below canopy (line 417) and relative variations in concentration levels of OH, MT and O3 (line 337-344).

What's the time resolution of data in Fig. 2b and 2d, there seem to be much less data than those in Fig. 2c.

Q in panels (b) and (d) were calculated for those periods for which the growth rate of particles was possible to determine. In panel (c) all the monoterpene measurements are presented, and those corresponding with events of determined growth rate are encircled. We have added an explanation to caption of Figure 2 to explain the reason for the different data points that are displayed in the panels.

Page 27151 line 27, "An overall C loss of 100 PgC assumed to be in the form of CO2 ", what's the reference year?

Added clarification (compared to today's levels; seen also in Table 1; line 353).

Table 1: what's the unit of "NPP_global"?

Thanks, is clarified in the Table caption. (now Table 2)

To improve the readability, "BVOC in Tg C a-1", should be "BVOC emissions" also correct that in the table. For the unit "ug_C g-1 h-1", what's the meaning of subscript "C" (instead of C in Pg C)? Overall, it is difficult to connect the table with its caption.

We have removed the subscript format in "C". The table caption was edited (also in response to reviewer one), and we hope it is easier to read noWew.

Table 2: The paper is an assessment of competing effects of CO2 and SOA. The negative forcing of SOA effect has been evaluated and given. For comparison, what's the forcing due to a change of CO2?

Table is now Table 3. Since CO2 is a well-mixed greenhouse gas its value can only be given globally and is stated in the text (403). We feel it would look odd to add this single number into the table. Moreover, we were severely criticized in an earlier version of the manuscript for over-interpreting our radiative forcing estimates, which is why we would prefer to leave the table unchanged.

Figure 1: For "maximum summer leaf area index", do you refer to seasonal, monthly or daily data? "a,b" are used in the figure caption while "A,B" are used in figure labeling.

Thanks, we clarified. We also use capital letters for Figure and caption.

Figure 3: "Areas with statistical significant changes in CCN are indicated.", can you elaborate on the statistical analysis?

The figure 3 right panel indicates areas with significant changes with dots. The statistical analysis is based on monthly average CCN concentrations from 5-years of simulated data, and statistical significance of the CCN anomaly is evaluated using a two-sample t test, without assuming equal variance between the two populations. Added explanatory text to the Figure caption.

Figure 4: Can you also show the absolute increase (in the supplement) for reference?

Showing absolute changes in SOA mass in different size modes is unfortunately not possible from our analysis, since aerosol masses and the respective changes are dominated by accumulation and coarse modes, whereas the climate effects would be sensitive to new CCN from growth from nucleation and Aitken mode. However, we revised the Figure caption of fig. 4 to add more detail.

Figure A1: CO2 on/off labels seem missing in top panels.

That is intentional, since the CO2 inhibition is compared to today's atmospheric CO2 as a reference = simulations with on and off would not show a large difference; the difference becomes only visible in the future simulations. Is clarified in the revised figure caption.

References:

Hens, K., Novelli, A., Martinez, M., Auld, J., Axinte, R., Bohn, B., Fischer, H., Keronen, P., Kubistin, D., Nölscher, A. C., Oswald, R., Paasonen, P., Petäjä, T., Regelin, E., Sander, R., Sinha, V., Sipilä, M., Taraborrelli, D., Tatum Ernest, C., Williams, J., Lelieveld, J., and Harder, H.: Observation and modelling of HO_x radicals in a boreal forest, Atmos. Chem. Phys., 14, 8723-8747, doi:10.5194/acp-14-8723-2014, 2014.

Nieminen, Tuomo, et al. "Trends in atmospheric new-particle formation: 16 years of observations in a boreal-forest environment." *Boreal Environment Research* 19 SB (2014)

Petäjä, T., Mauldin, III, R. L., Kosciuch, E., McGrath, J., Nieminen, T., Paasonen, P., Boy, M., Adamov, A., Kotiaho, T., and Kulmala, M.: Sulfuric acid and OH concentrations in a boreal forest site, Atmos. Chem. Phys., 9, 7435-7448, doi:10.5194/acp-9-7435-2009, 2009.

Sellegri, K., Hanke, M., Umann, B., Arnold, F., and Kulmala, M.: Measurements of organic gases during aerosol formation events in the boreal forest atmosphere during QUEST, Atmos. Chem. Phys., 5, 373-384, doi:10.5194/acp-5-373-2005, 2005.

Future vegetation-climate interactions in Eastern Siberia: an assessment of the competing effects of CO_2 and secondary organic aerosols

A Arneth[1,*], R Makkonen[2], S Olin[3], P Paasonen[2], T Holst[3], MK Kajos[2], M Kulmala[2], T Maximov[4], PA Miller[3], G. Schurgers[3,5]

[1] Karlsruhe Institute of Technology, Institute of Meteorology and Climate Research/Atmospheric Environmental Research, Garmisch Partenkirchen, Germany

[2] Department of Physics, University of Helsinki, P.O. Box 64, 00014 University of Helsinki, Finland

[3] Department of Physical Geography and Ecosystem Science, Lund University, Sölvegatan 12, 22362 Lund, Sweden

[4] Department of Plant Ecological Physiology and Biochemistry Lab., Institute for Biological Problems of Cryolithozone SB RAS, 41, Lenin ave, Yakutsk 677980, Russia

[5] Department of Geosciences and Natural Resource Management, University of Copenhagen, Øster Voldgade 10, 1350 Copenhagen, Denmark

*: almut.arneth@kit.edu

Abstract

Disproportional warming in the northern high latitudes, and large carbon stocks in boreal and (sub)arctic ecosystems have raised concerns as to whether substantial positive climate feedbacks from biogeochemical process responses should be expected. Such feedbacks occur if increasing temperatures lead to e.g., a net release of CO_2 or CH_4. However, temperature-enhanced emissions of biogenic volatile organic compounds (BVOC) have been shown to contribute to the growth of secondary organic aerosol (SOA) which is known to have a negative radiative climate effect. Combining measurements in Eastern Siberia with model-based estimates of vegetation and permafrost dynamics, BVOC emissions and aerosol growth, we assess here possible future changes in ecosystem CO_2 balance and BVOC-SOA interactions, and discuss these changes in terms of possible climate effects. ~~On global level~~Globally, the effects of changes in Siberian ecosystem CO_2 balance and SOA formation ~~, both~~ are ~~very~~ small, but when concentrating on Siberia and the northern hemisphere the negative forcing from changed aerosol direct and indirect effects become notable – even though the associated temperature response would not necessarily follow a similar spatial pattern. While our analysis does not include other important processes that are of relevance for the climate system, the CO_2 and BVOC-SOA interplay ~~used~~ serves as an example ~~of~~ for the complexity of the interactions between emissions and vegetation dynamics that underlie individual terrestrial feedbacks and highlights the importance of addressing ecosystem-climate feedbacks in consistent, process-based model frameworks.

1. Introduction

Warming effects on ecosystem carbon cycling in northern ecosystems (Serreze et al., 2000;Tarnocai et al., 2009), and the potential for large climate-feedbacks from losses of CO_2 or CH_4 from these carbon-dense systems have been widely discussed (Khvorostyanov et al., 2008; Schuur et al., 2009; Arneth et al., 2010). Other biogeochemical processes can also lead to feedbacks, in particular through emissions of biogenic volatile organic compounds (BVOC) that are important precursors for tropospheric O_3 formation, affect methane lifetime and also act as precursors for secondary organic aerosol (SOA). These latter interactions with SOA have a cooling effect (Arneth et al., 2010; Makkonen et al., 2012b; Paasonen et al., 2013). Condensation of monoterpenes (*MT*), a group of BVOC with large source strength from coniferous vegetation, on pre-existing particles increases the observed particle mass, as well as the number of particles large enough to act as cloud condensation nuclei (CCN; equivalent to particles > *ca.* 100 nm) at boreal forest sites (Tunved et al., 2006). For present-day conditions, Spracklen et al. (2008a) estimated a radiative cooling of -1.8 to -6.7 W per m^{-2} of boreal forest area from the BVOC-SOA interplay.

How future changes in *MT* emissions affect SOA growth and climate is very uncertain. This is partially because of the lack of process-understanding of the various steps of aerosol formation and growth, and interactions with cloud formation (Hallquist et al., 2009; Carslaw et al., 2010), and partially because the issue of how spatial patterns of changing emissions of atmospherically rapidly reactive substances translate into a changing patterns of radiative forcing, and then into a surface temperature change, has not yet been resolved (Shindell et al., 2008; Fiore et al., 2012).

The Russian boreal forest represents the largest continuous conifer region in the world. About one third of this forested area (ca. 730 X 10^6 ha) is dominated by larch (Shvidenko et al., 2007), in particular by the *Larix gmelinii* and *L. cajanderii* forests growing east of the Yenisei river on permafrost soils. Despite its vast expanse, the first seasonal measurements of *MT* emissions from Eastern Siberian larch have only recently been published (Kajos et al., 2013). Leaf *MT* emission capacities are highly species-dependent, thus any model estimate of *MT* emissions from boreal larch forests that rely solely on generic BVOC emission parameterisations obtained from other conifer species will give inaccurate emission and related SOA aerosol number concentrations for this region (Spracklen et al., 2008a). We therefore provide here a first assessment of *MT* emission rates from the Eastern Siberian larch biome, combining measured emission capacities with a process-based dynamic vegetation model and quantitatively linking *MT* emissions and SOA formation. We use the observations and process-models to assess climate change effects on future vegetation composition, BVOC emissions and the concentration of particles of CCN size. We discuss how the climate impact of future SOA levels from changes in BVOC emissions across Eastern Siberia compares with changes in the regional CO_2 balance. The chief goal of the study was not to provide a full surface climate-feedback quantification (for which today's global coupled modelling-tools are insufficient) but rather to highlight the number of potentially opposing processes that need to be covered when doing so.

2. Methods

2.1 Site description, BVOC and aerosol measurements

Leaf BVOC emissions fluxes, above canopy monoterpene concentration and aerosol particle size and number concentration were measured during the growing season 2009 at the research station Spasskaya Pad, located ca. 40km to the northeast of Yakutsk (62°15'18.4"N, 129°37'07.9"E) and centred in the Eastern Siberian larch biome (Kobak et al., 1996;Tchebakova et al., 2006). In the northern direction, no major pollution sources exist within hundreds of km, the nearest mining areas are concentrated to the south and west of Yakutsk. The predominant air flow to the site is either from southern (via Yakutsk) or northern locations. Forest fires contribute to aerosol load in summer.

An eddy covariance tower for measurements of forest-atmosphere exchange of CO_2, water vapour and sensible heat was established at Spasskaya Pad in the late 1990s (Ohta et al., 2001;Dolman et al., 2004) in a *L. cajanderii* forest growing on permafrost soil with an understory vegetation consisting of ericaceous shrubs. The forest has an average age of ca. 185 years and canopy height is little less than 20 m. Maximum one-sided larch leaf area index in summer is around two (Ohta et al., 2001, Takeshi et al., 2008). In 2009, leaf samples for BVOC analyses were taken, accessing the upper part of the canopy from a scaffolding tower located within few hundred metres of the eddy flux tower (Kajos et al., 2013). Using a custom-made Teflon branch chamber, air filtered of O_3 was sampled onto Tenax-TA/Carbopack-B cartridges with a flow rate of 220 ml min^{-1}. A total of 5-12 samples were taken during the day, from two trees on south-facing branches approximately 2 m below the tree top. The cartridge samples were stored at 5°C during the campaigns, transported afterwards to Helsinki and thermally desorbed and analysed using a thermal desorption instrument (Perkin-Elmer TurboMatrix 650, Waltham, USA) attached to a gas-chromatograph (Perkin-Elmer Clarus 600, Waltham, USA). For details on

chamber, adsorbents and laboratory measurements, see (Haapanala et al., 2009;Ruuskanen et al., 2007;Hakola et al., 2006).

Monoterpene concentrations and forest-atmosphere exchange fluxes were measured with a high-sensitive Quadrupole PTR-MS (Ionicon, Innsbruck, Austria) located in a hut at the foot of the eddy covariance tower. Sample air was drawn through a heated PFA tube using a 20 l min-1 flow from the inlet located at 30.3m above ground. While reporting here on monoterpenes only, a range of masses, corresponding to BVOCs (e.g., isoprene, methanol, acetaldehyde-) were sampled sequentially, with typical dwell times of 0.5 s and scanning sequences of around 4s. Measurement set-up, disjunct eddy covariance flux calculations, and quality control followed Holst et al. (2010). It was not possible to import a gas calibration standard to Spasskaya Pad due to security and customs restrictions, and thus the PTR-MS could not be calibrated on-site. However, the instrument had been calibrated before and after the field campaign using a gas standard mixture from Ionimed (Innsbruck, Austria) using the same detector and instrument settings as during the field campaigns.

Aerosol particles were continuously monitored with a Scanning mobility particle sizer (SMPS) located at the foot of the eddy covariance tower, connected to a Differential mobility analyzer (DMA; Hauke type: medium; custom built; for size segregation of aerosol particles) in front of a Condensation Particle Counter (CPC; 3010, TSI Inc. USA; for determining the number of the size segregated particles). The system was identical to the one described and evaluated in (Svenningsson et al., 2008). Scans across the size range of 6 – 600 nm were completed every 5 minutes. The SMPS data were used to determine occasions of aerosol particle nucleation. The growth rates were calculated from log-normal modes fitted to the measured particle size distribution following Hussein et al. (2005). The time evolution of the diameters at which the fitted modes peaked was inspected visually, and the growth rate was determined with linear least squares fitting to these peak diameters whenever a continuous increase in diameter was observed. In this analysis we calculated growth rates for particles from 25 to 160 nm.

The source rate for condensing vapour (Q, molecules cm^3 s^{-1}) was determined by calculating the concentration of condensable vapour needed to produce the observed growth rate (C_{GR}, cm^{-3}, Nieminen et al., 2010) and the condensation sink from the particle size distribution (CS, s^{-1}, Kulmala et al., 2001). In steady state the sources and sinks for the condensing vapour are equal, and thus we determined the source rate as $Q=C_{GR}\bullet CS$.

2.2 Modelling of dynamic vegetation processes, permafrost and BVOC emissions

We applied the dynamic global vegetation model (DGVM) LPJ-GUESS (Smith et al., 2001; Sitch et al., 2003), including algorithms to compute canopy BVOC emission following (Niinemets et al., 1999;Arneth et al., 2007b;Schurgers et al., 2009a), and permafrost as adopted from Wania et al. (2009) (Table 1). LPJ-GUESS simulates global and regional dynamics and composition of vegetation in response to changes in climate and atmospheric CO_2 concentration. Physiological processes like photosynthesis, autotrophic and heterotrophic respiration are calculated explicitly, a set of carbon allocation rules determines plant growth. Plant establishment, growth, mortality, and decomposition, and their response to resource availability (light, water) modulate seasonal and successional population dynamics arising from a carbon allocation trade-off (Smith et

al., 2001). Fire disturbance is included in the model (Thonicke et al., 2001). Similar to other DGVMs, a number of plant functional types (PFT) are specified to represent the larger global vegetation units (Sitch et al., 2003).

BVOC emissions models, whether these are linked to DGVMs or to a prescribed vegetation map, all rely on using emission potentials (*E**, leaf emissions at standardised environmental conditions) or some derivatives in their algorithms. In LPJ-GUESS, production and emissions of leaf and canopy isoprene and monoterpenes are linked to their photosynthetic production, specifically the electron transport rate, and the requirements for energy and redox-equivalents to produce a unit of isoprene from triose-phosphates (Niinemets et al., 1999; Arneth et al., 2007b; Schurgers et al., 2009a). A specified fraction of absorbed electrons used for isoprene (monoterpene) production (ε) provides the link to PFT-specific *E** (Arneth et al., 2007a); in case of monoterpenes emitted from storage an additional correction is applied to account for their light-dependent production (taking place over parts of the day) and temperature-driven (taking place the entire day) emissions (Schurgers et al., 2009a). Half of the produced monoterpenes were stored, whereas the other half was emitted directly (Schurgers et al., 2009a). Values for *E** similar to the global parameterisation for most of the model's PFTs (Schurgers et al., 2009a), with exception of boreal needle-leaf summergreen (BNS) "larch" PFT (see results).

Contrasting the ~~Leaf BVOC emissions are stimulated~~ stimulation of BVOC emissions in a ~~future~~ warmer and more productive environment~~, in response to warmer temperatures. Moreover, warmer temperatures and CO_2 fertilisation of photosynthesis lead to enhanced vegetation productivity and leaf area, with additional positive effects on BVOC emissions. But~~ higher CO_2 concentrations have ~~also~~ been shown to inhibit leaf isoprene production. Even though the underlying metabolic mechanism is not yet fully understood, this effect has been observed in a number of studies (for an overview see Figure 6 in Arneth et al., 2011). Due to limited experimental evidence, whether or not a similar response occurs in monoterpene producing species cannot yet be confirmed, especially in species that emit from storage. The model is set-up to test this hypothesis. Arneth et al. (2007a) proposed an empirical function for CO_2-inhibition, based on the ratio of leaf internal CO_2 concentration at a standard atmospheric CO_2 level (taken as 370ppm) and at the given atmospheric CO_2 levels of the simulation year (both calculated for non-water-stressed conditions); the relationships has been shown since to fit an updated compilation of observations well (Arneth et al., 2011). The algorithm that describes the CO_2-inhibition of BVOC emission can either be enabled or disabled in the model (Arneth et al., 2007a) and simulations results thus compared (see Figure A1, Appendix; Table 2).

~~Monoterpene compounds can be emitted either directly following their synthesis in the chloroplast, in an "isoprene-like" fashion, or from storage pools, resulting in an emission pattern that is independent of light availability. The observed emissions of monoterpenes by larch possibly exhibit a hybrid between emission directly after synthesis in the chloroplast and emission from storage pools, as has also been found for other coniferous species (Schurgers et al., 2009a). The needle-level measurements by Kajos et al. (2013) on larch indicated a combined light- and temperature response, even though a robust differentiation to a temperature-only model was not possible due to the limited sample size. An earlier study by Ruuskanen et al. (2007) on a 5-year old *L. sibirica* tree indicated a better performance of the temperature-only emission model for monoterpene species compared to the light and temperature approach. In the model simulations performed~~

here, half of the produced monoterpenes were stored, whereas the other half was emitted directly (Schurgers et al., 2009a).

LPJ-GUESS is a second generation DGVM (Fisher et al., 2010) and includes plant demography, such that forest successional dynamics and competition for water and light between individual age cohorts are treated explicitly (Smith et al., 2001). The forest growth dynamics thus differentiate between early successional, short-lived species that invest in rapid growth and shade-tolerant trees with resource allocation aimed towards longer-lived growth strategies. As a result, the model's PFTs can be mapped to tree species when required information for model parameterisation is available. This feature provides a distinct advantage when applying the necessary BVOC emission capacities that are based on species (rather than functional-type) average values (Arneth et al., 2008;Schurgers et al., 2009b;Niinemets et al., 2010). Larch, in this model setup would be represented by the shade-intolerant boreal needle-leaf summergreen (BNS) PFT, and for other PFTs the global parameterisation was used (Schurgers et al., 2009a).

LPJ-GUESS was recently expanded with a permafrost module following Wania et al. (Wania et al., 2009;Miller and Smith, 2012) in which a numerical solution of the heat diffusion equation was introduced. The soil column in LPJ-GUESS now consists of a snow layer of variable thickness, a litter layer of fixed thickness (5 cm), and a soil column of depth 2 m (with sublayers of thickness 0.1 m) from which plants can extract non-frozen water above the wilting point. A "padding" column of depth 48 m (with thicker sublayers) is also present beneath these three layers to aid in the accurate simulation of temperatures in the overlying compartments (Wania et al., 2009). Soil temperatures throughout the soil column are calculated daily, and change in response to changing surface air temperature and precipitation input, as well as the insulating effects of the snow layer and phase changes in the soil's water.

Here we run the model with 0.5 degree spatial resolution, using climate and atmospheric CO_2 as driving variables as described in the literature (Smith et al., 2001). Values describing growth and survival of ~~for~~ the BNS ~~BNS~~ "larch" PFT were adopted from previous studies (Sitch et al., 2003; Hickler et al., 2012; Miller and Smith, 2012), but with the degree-day cumulative temperature requirements on a five-degree basis (GDD5) to attain full leaf cover reduced from 200 to 100 (Moser et al., 2012). Minimum GDD5 to allow establishment was set to 350 resulting in establishment of seedlings in very cold locations. Soil thermal conductivity was 2 $Wm^{-1} K^{-1}$. ~~The modelled distribution of larch in LPJ-GUESS (Figure 1) compares well with observation-based maps (Wagner, 1997).~~ The model was spun up for 500 years to 1900 values using CO_2 concentration from the year 1900 and repeating de-trended climate from 1901-1930 from CRU (Mitchell and Jones, 2005). Historical (20^{th} century) simulations used observed CO_2 concentrations and based on variable CRU climate. Simulations for the 21^{st} century were based on ECHAM climate, using RCP 8.5 emissions (Riahi et al., 2007). The model requires daily radiation, precipitation and maximum and minimum air temperatures as input (Arneth et al., 2007b). The generated GCM climate was interpolated to the CRU half-degree grid, and monthly values interpolated to daily ones (see Ahlström et al., 2012, and references therein). These daily fields were then bias-corrected using the years 1961-1990 as reference period, as in Ahlström et al. (2012). CO_2 inhibition of BVOC emissions were switched on and off in separate simulations to assess the sensitivity of our results to this process. Totals across Siberia were calculated for a grid-box that ranged from 46 to 71 ^{o}N and 76 to 164 ^{o}E.

Simulated changes in total carbon uptake or losses were translated into radiative forcing following (IPCC, 2007), assuming a 50% uptake in oceans in case of a net loss to the atmosphere (Sitch et al., 2007).

2.3 Modelling aerosols and CCN

To model the effect of BVOCs on CCN concentrations, we use the global aerosol-climate model ECHAM5.5-HAM2 (Zhang et al., 2012). ECHAM5.5-HAM2 includes the aerosol components of black carbon, organic carbon, dust, sea salt and sulfate (Table 1) , and describes the aerosol size distribution with seven log-normal modes. The microphysics module M7 (Vignati et al., 2004) includes nucleation, coagulation and condensation. In this study, we use the ECHAM5.5-HAM2 version with activation-type as described in Makkonen et al. (Makkonen et al., 2012). For simulating secondary organic aerosol, we use the recently developed SOA module (Jokinen et al., 2015). The SOA module explicitly accounts for gas-phase formation of extremely low volatility organic compounds (ELVOCs) from monoterpene oxidation. The module implements a hybrid mechanism for SOA formation: ELVOCs are assumed to condense to the aerosol population according to the Fuchs-corrected condensation sink, while semi-volatile organic compounds (SVOCs) are partitioned according to organic aerosol mass. While simulated ELVOCs are able to partition more effectively to nucleation and Aitken mode, hence providing growth for nucleated particles to CCN size, SVOCs primarily add organic mass to accumulation and coarse aerosol modes. A total SOA yield of 15% from monoterpenes is assumed (Dentener et al., 2006). While similar assumption on total SOA yield is applied by most aerosol-climate models, the simulated SOA is likely to be underestimated (e.g., Tsigaridis et al., 2014).

~~Whether or not BVOCs can increase the availability of cloud condensation nuclei (CCN) depends on the availability of sub-CCN sized particles (O'Donnell et al., 2011). Anthropogenic primary emissions are introduced to the model as 60 nm particles, hence condensation of sulfuric acid and organic vapours is generally needed in order to grow these particles to CCN sizes. In Siberia, the modelled primary particle emissions are dominated by wildfires, which are assumed to inject large particles with 150 nm diameter. The model is using T63 spectral resolution with 31 vertical hybrid sigma levels.~~

ECHAM5.5-HAM2 was run with different BVOC emission scenarios in year 2000 and 2100 simulated offline with LPJ-GUESS (see previous section). The model is using T63 spectral resolution with 31 vertical hybrid sigma levels. The simulations apply present-day oxidant fields as in Stier et al. (2005). ~~The assumption of unchanging oxidant fields induces some uncertainty for future simulations and inconsistency with present-day simulations with varying biogenic emissions, since both anthropogenic and biogenic emissions are likely to modify the atmospheric oxidative capacity.~~ All simulations are initiated with a six months spin-up, followed by 5 years of simulation for analysis. The model climate is nudged towards ERA-40 reanalysis year 2000 meteorology, an approach that is widely used in aerosol-climate assessments (Zhang et al., 2014). ~~Nudging towards reanalysis meteorology establishes evaluation of BVOC-aerosol coupling with unchanged meteorological fields, but restricts the model in terms of aerosol-climate feedbacks, since e.g., nudging future climate simulations with present-day meteorological winds is based on the assumption that e.g. cloudiness, or wind direction and –speed etc. are not changing.~~ Present-day wildfire and

anthropogenic aerosol and precursor emissions are applied for all simulations (Dentener et al., 2006). One of the foci here are BVOC, comparing present-day and future BVOC emissions (choosing a conservative estimate of ~~with~~ E^*=1.9 μg C m^{-2}(leaf) h^{-1}, see results section for further detail on E^* but keeping other emissions constant (oxidant fields and nudging meteorology are same for both 2000 and 2100). The emissions of dust and sea salt are modelled interactively (Zhang et al., 2012).

The analysis of model results includes total particle number concentration (CN) and cloud condensation nuclei at 1% supersaturation (CCN(1%)), since it reflects the changes in Aitken mode concentrations and local changes in precursor emissions. While "realistic" supersaturations are generally lower, choosing CCN(1.0%) concentration provides the upper limit for CCN concentrations. The simulations are also used to assess the radiative effects of SOA. In the simulations, the aerosol concentrations are interactively coupled to the cloud-microphysics scheme (Lohmann et al., 2007) and to the direct aerosol radiative calculation. The aerosol indirect effect is evaluated as a change in cloud radiative forcing (ΔCRF). The direct aerosol effect accounts only for clear-sky short-wave forcing (ΔCSDRF). The radiative effects are calculated as differences from two time-averaged 5-year simulations as

$$\Delta CRF = CRF(BVOC_{2100}) - CRF(BVOC_{2000})$$

$$\Delta CSDRF = CSDRF(BVOC_{2100}) - CSDRF(BVOC_{2000}).$$

Subscripts "2000" and "2100" denotes that BVOC emissions from this year were used, while other model conditions were based on present-day values.

3. Results

3.1 Present-day expanse of larch forest and BVOC emissions

~~Larch, in this model setup would be represented by the shade-intolerant boreal needle-leaf summergreen (BNS) PFT, and for other PFTs the global parameterisation was used (Schurgers et al., 2009a).~~

~~The dynamic global vegetation model~~ LPJ-GUESS reproduces the present-day circumpolar permafrost distribution (Figure 1; shown as circumpolar map for comparison with Tarnocai et al (2009)) and, with the exception of the Kamchatka peninsula, simulates also the expanse of the larch-dominated forests in Eastern Siberia (Figure 1; Miller and Smith, 2012, Wagner, 1997). Maximum leaf area index (LAI) calculated by the model for the Spasskaya Pad forest (62°15'18.4"N, 129°37'07.9"E, 220 m a.s.l), where the BVOC measurements were obtained, was 2.0 (averaged over years 1981-2000; not shown), and is in good agreement with the measured values during that period (1.6; Takeshi et al., 2008). Total present-day modelled soil C pools over the top 2 m in Eastern Siberia are 216 Gt C, and 454 Gt C for circumpolar soils summed for latitudes above 40°N (Table 2). A recent estimate of C stored in northern latitude soils affected by permafrost was 191, 495, and 1024 Gt C in the 0-30, 0-100 and 0-300 cm soil layer, based on extrapolating observations stored in the Northern Circumpolar Soil Carbon Database (Tarnocai et al., 2009). These numbers indicate that the values calculated with LPJ-GUESS are lower than observation-based ones, most likely underestimating C-density in particular in the soil layers below few tenths of cm.

~~For the "larch" plant functional type in LPJ-GUESS (Schurgers et al., 2009a), an emission potential of E^*= 2.4 μg C m^{-2}(leaf) h^{-1} was adopted in previous simulations from Guenther et al., (1995), a recommendation that at that time did not include observations from any larch species.~~

Kajos et al. (2013) measured for the first time *MT E** from *L. cajanderii.* Their measurements, taken over an entire growing season at Spasskaya Pad, suggested values of E^* ranging from 1.9 μg C m^{-2}(leaf) h^{-1} at the lower end, to 9.6 μg C m^{-2}(leaf) h^{-1} at the upper. Applying a weighted measured-average E^* of 6.2 μg C m^{-2} (leaf) h^{-1} , in LPJ-GUESS led to average summer daily monoterpene emissions of 2.9 (± 0.8, 1 standard deviation, June) mg C m^{-2} d^{-1}, and 2.2 (± 0.8, July) mg C m^{-2} d^{-1} for the gridlocation representing the Spasskaya Pad site, and for the same year of measurements than reported in Kajos et al (2013). These values are within 25 and 10% of measured values (3.3 ± 2.9 mg C m^{-2} d^{-1}, June; 2.4 ± 1.6 mg C m^{-2} d^{-1}; July), even though the modelled day-to-day variation was smaller which is expected when applying grid-averaged climate as model input. By comparison, for a boreal Scots pine forest in southern Finland average June and July monoterpene emissions were somewhat larger than the values for larch (3.8 and 5.1 mg C m^{-2} d^{-1}, respectively; Rantala *et al.*, 2015). For a Larix kaempferi-dominated temperate forest in Japan, Mochizuki et al (2012) extrapolated, based on their measurements, summer time maxima of ca. 10 mg C m^{-2} d^{-1} .

Across the Siberian larch biome applying E^* of 6.2 μg C m^{-2} increased simulated total present-day *MT* emissions ~~across the Siberian larch biome~~ from 0.11 $TgCa^{-1}$ (as in Schurgers et al., 2009a) to 0.21 $TgCa^{-1}$, or to 0.42 $TgCa^{-1}$ when the maximum E^* was used (~~Table 1~~Table 2). The observed range in E^*, and the calculated range in total emissions across Siberia, might reflect variability in tree microclimate or genetic variability, or ~~was~~ might have been induced by (undetected) mechanic or biotic stress during the time of measurements (Staudt et al., 2001; Bäck et al., 2012; Kajos et al., 2013). While our data are insufficient to make a finite suggestion of *L. cajanderi E**, the measurements provide evidence for potentially substantially higher *MT* emissions from Siberian larch than previous estimates.

3.2 Present-day aerosols, and links to BVOC

New particle formation events (Figure 2a) were observed regularly at Spasskaya Pad. The calculated volumetric source rates of condensing vapours (Q), the product of vapour concentration required for the observed particle growth rate and particle loss rate (Kulmala et al., 2005), increased exponentially with temperature (Figure 2b). *MT* concentrations increased with temperature as well, with a slope relatively similar to that found for the Q *vs.* T relationship (Figure 2c). Consequently, a positive relationship emerged between Q and *MT* concentration (Figure 2d), which supports previous field and laboratory evidence that *MT* and their oxidation products are a main precursor to the observed particle formation and growth.

Figure 2d shows the connection between the BVOC concentration and the formation rate of vapours causing the growth of the aerosol particles. Even though the monoterpene concentrations were measured above and the aerosol growth rates below the canopy, the observed correlation indicates that BVOC concentration is an important contributor to the regional aerosol growth and supports the theory that the condensation of organic vapour is largely responsible for the formation of secondary organic aerosol (Hallquist et al., 2009, Carslaw et al., 2010). Substantial within-canopy chemical reactions would be expected to worsen the relationship. The

correlation depicted in Figure 2d is determined in particular by the the formation of secondary organic aerosol on pre-existing aerosol particles, whereas the nucleation rate of new aerosol particles seems not to be dominated by the landscape-scale emissions and surface concentrations of BVOCs. For instance, most nucleation events in a Scots pine dominated landscape in Finland have been found in spring, when measured monoterpene concentrations in the near-surface were about one tenth of the summer time maximum (ca. 60 ppt, *vs*. up to 500 ppt; Haapanala et al., 2007; Lappalainen et al., 2009). We found here MT concentrations of similar magnitude to these.

By contrast to temperature and BVOC concentrations, levels of radiation, which can be considered a surrogate for the concentration of the OH radical (OH•), did not affect *Q* (Figure 2b), even though OH• has been considered an important player for aerosol formation. Rohrer and Berresheim (2006) showed a strong correlation between solar ultraviolet radiation and OH• concentration at the Hohenpeissenberg site in Germany. Furthermore, Hens et al. (2014) demonstrated that the day-time OH• concentrations in (especially) boreal forest depend on solar radiation, both above and below the canopy. Hence, the poor relation between the source rate of condensing vapour and orders-of-magnitude variation in levels of radiation (Fig. 2b) indicates that OH-radical concentration did not have a major impact on Q. This agrees with the findings by Ehn et al. (2014) that ozone instead of OH• is an important, if not the main, atmospheric agent oxidising organic vapours into a chemical form that condenses on particle surfaces. Since the relative variation in ozone concentrations is much smaller than in BVOC (or OH) concentrations (Hens et al., 2014), the similarity in the dependencies of Q and MT concentration and temperature (Figures 2b and 2c) are in favour of a more significant role of ozone than of OH in the formation of condensable vapours. In general~~Thus~~, our results indicate that factors and processes besides the concentrations of SO_2 and OH• seem to limit aerosol production in non-polluted environments (Kulmala et al., 2005).

3.3 Future carbon pools, vegetation distribution and BVOC emissions in Siberia

In a warmer environment with higher atmospheric CO_2 levels, the simulations indicated drastically reduced area of permafrost in Siberia (Figure 1). Total net primary productivity in the simulated domain increased from an annual average of 3.5 PgC a^{-1} to 5.9 PgC a^{-1} at the end of the 21st century. An overall C loss of 100 PgC assumed to be in the form of CO_2 (since the model does not yet include a dynamic surface hydrology which would be necessary to assess changing methane emissions) at the end of the 21st century, compared to present-day conditions, was calculated from the shrinking Siberian areas of permafrost (~~Table 1~~Table 2). However, warming and higher levels of atmospheric CO_2 led also to increasing LAI, and to larch-dominated areas showing the expected north- and north-eastwards shift (Figure 1) compared to present-day climate (Miller and Smith, 2012). The carbon uptake in expanding vegetation into permafrost-free areas, combined with enhanced productivity across the simulation domain overcompensates for the losses from C-pools in permafrost areas (~~Table 1~~Table 2).

Without CO_2 inhibition of BVOC emissions f~~F~~uture *MT* emissions were, as expected, notably enhanced: directly as a result of warmer leaves, ~~and~~ but augmented by the future higher LAI of larch and evergreen conifers (Figure 1D; ~~Table 1~~Table 2, Figure A1). Since the emissions scale with the emission factors applied,

the proportional increase between present-day and future climate conditions is independent of the value of *E**. Whether or not leaf *MT* emissions are inhibited by increasing atmospheric CO_2 levels to similar degree to what was found for isoprene is difficult to assess from today's limited number of studies (e.g., Niinemets et al., (2010), and references therein). We included both simulation results in Table 2 since ~~S~~similarities in the leaf metabolic pathways of isoprene and *MT* production suggest such an inhibition, but possibly this effect does not become apparent in plant species where produced *MT* are stored unless the storage pools become measurably depleted by the reduced production. By contrast, species emitting *MT* in an "isoprene-like" fashion immediately after production should more directly reflect CO_2 inhibition. Evergreen conifers typically emit most *MT* from storage pools, although recent experiments have shown that some light-dependent emissions also contribute to total emission fluxes. Accordingly, based on the leaf-level measurements, larch could follow a hybrid pattern between emission after production and from storage (Kajos et al., 2013). Without accounting for CO_2 inhibition, *MT* emissions across the model domain more than doubled (Figure 1; ~~Table 1~~Table 2) by 2100, as a consequence of higher emissions per leaf area due to warmer temperatures, and of the larger emitting leaf area in response to higher photosynthesis. With –CO_2 inhibition included, simulated changes were negligible, similar to what was shown in previous BVOC simulations with the model (Arneth et al.,2007a; Arneth et al., 2008).

4. Discussion

Boreal vegetation has been shown to respond to the recent decades' warming and increasing atmospheric CO_2 levels with a prolonged growing season and higher maximum LAI, similar to patterns in our simulations (Piao et al., 2006). The calculated enhanced biomass growth is in-line with experimental evidence of higher C in plant biomass in warming plots at tundra field sites (Elmendorf et al., 2012;Sistla et al., 2013). In Siberian mountain regions, an upward movement of vegetation zones has been recorded already (Soja et al., 2007), while the analysis of evergreen coniferous undergrowth abundance and age shows spread of evergreen species, especially *Pinus siberia*, into Siberian larch forest (Kharuk et al., 2007). These observations thus support the modelled shift in vegetation zones, and change in vegetation type composition and productivity. Likewise, other models with dynamic vegetation also have shown a strong expansion of broadleaved forests at the southern edge of the Siberian region in response to warming (Shuman et al., 2015).

Warming and thawing of permafrost soils is being observed at global monitoring network sites, including in Russia (Romanovsky et al., 2010). Estimates of carbon losses from northern wetland and permafrost soils in response to 21st century warming range from a few tens to a few hundreds Pg C, depending on whether processes linked to microbial heat production, thermokarst formation and surface hydrology, winter snow cover insulation, dynamic vegetation, C-N interactions, or fire are considered (Khvorostyanov et al., 2008;Schuur et al., 2009; Arneth et al., 2010; Koven et al., 2011; Schneider von Deimling et al., 2012). For instance, a modelled range of 0.07 - 0.23 Wm^{-2} forcing associated with a 33 - 114 $PgCO_2$-C loss from permafrost regions was found for a simulation study that was based on the RCP 8.5 climate and CO_2 scenarios, but excluding full treatment of vegetation dynamics (Schneider von Deimling et al., 2012). In a recent literature review, Schaefer et al (2014) found a range from cumulative 46 to 435 CO_2 –equivalents (accounting for CO_2

and CH_4), or 120 ± 85 GtC by 2100 in response to different future warming scenarios and modelling approaches. In our simulation, the CO_2-C loss from the decreasing Siberian permafrost region would be equivalent to a 0.13 additional Wm^{-2} forcing in 2100 (see methods). Likely, this number is too low since the model does not include thermokarst processes, which can facilitate rapid thaw (Schaefer et al., 2014, and references therein). The modelled carbon loss was offset when taking into account vegetation dynamics and processes across the entire Siberian study-domain (~~Table 1~~Table 2), including a shift in PFT composition, and enhanced productivity especially in the southern regions, such that the overall carbon uptake including enhanced net primary productivity and expanding woody vegetation resulted in a small negative (-0.09 Wm^{-2}) effect.

LPJ-GUESS is a second generation DGVM (Fisher et al., 2010) and includes plant demography, such that forest successional dynamics and competition for water and light between individual age-cohorts are treated explicitly (Smith et al., 2001). The forest growth dynamics thus differentiate between early successional, short-lived species that invest in rapid growth and shade-tolerant trees with resource allocation aimed towards longer-lived growth strategies. As a result, the model's PFTs can be mapped to tree-species when required information for model parameterisation is available. The process-based treatment of resource competition such as for light and water has been shown to lead to a realistic growth response and distribution under present-day climate condition (Arneth et al., 1998; Schurgers er al., 2009b), which should also hold in future and past climates (Miller et al., 2008; Schurgers et al., 2009b). This feature also provides a distinct advantage when applying the necessary BVOC emission capacities that are based on species (rather than functional-type) average values (Arneth et al., 2008; Schurgers et al., 2009b; Niinemets et al., 2010). ~~For the "larch" plant functional type in LPJ-GUESS~~ In earlier simulations (Schurgers et al., 2009a), a~~n~~ generic emission potential of E^*= 2.4 µg C m^{-2}(leaf) h^{-1} was adopted for the BNS PFT ~~in previous simulations from~~based on a recommendation in Guenther et al., (1995), ~~a recommendation~~ that at that time did not include observations from any larch species. Here we demonstrate not only that a range of measured larch E^* (see Table 2) introduces large uncertainty in total MT emissions from Siberia, but also that it is fundamental to apply dynamic vegetation growth response (rather than static maps) for BVOC emissions estimates in changing environments.

Monoterpene compounds can be emitted either directly following their synthesis in the chloroplast, in an "isoprene-like" fashion, or from storage pools, resulting in an emission pattern that is independent of light availability. The observed emissions of monoterpenes by larch possibly reflect a hybrid pattern between emission directly after synthesis in the chloroplast and emission from storage pools, as has also been found for other coniferous species (Schurgers et al., 2009a). The needle-level measurements by Kajos et al. (2013) on larch indicated a combined light- and temperature response, even though a robust differentiation to a temperature-only model was not possible due to the limited sample size. An earlier study by Ruuskanen et al. (2007) on a 5-year old *L. sibirica* tree indicated a better performance of the temperature-only emission model for monoterpene species compared to the light and temperature approach.

Multiple interacting processes can alter monoterpene emissions in future. Irrespective of the relative roles of light *vs.* temperature dependence, ~~The temperature-dependency of monoterpene emissions, especially those~~

from stored pools, is a well-established response on the short-term. However, a change in *MT* concentrations and hence partial pressure in of *MT* in stored the storage pools, for instance in response to long-term warming, would affect emission capacities. Changes in measured *E** when investigated over the course of a growing season have been reported and could be related to a changing production rate (Niinemets et al., 2010). Likewise, observed profiles of *E** within tree canopies appear not only related to changes in leaf area-to-weight ratios along the canopy light and temperature gradients, but also to varying production rates (Niinemets et al., 2010). Emission capacities in *Q. ilex* leaves adapted to warm growth environment were notably enhanced (Staudt et al., 2003), but the experimental basis for an acclimation response of BVOC emissions to temperature remains remarkably poor (Penuelas and Staudt, 2010) and is indicative of the general lack of global modelling studies accounting for possibly acclimation of process responses to environmental changes (Arneth et al., 2012). In our simulations we aim to provide a range of a possible plastic BVOC-CO_2 response by switching the direct CO_2 inhibition on and off for both isoprene and monoterpene, but we do not account for other acclimation processes.

The assessment of climate effects of changes in the CO_2-C balance *vs* those of BVOC-SOA interactions is challenging, since the translation of regional changes in emissions of atmospherically reactive species into related radiative forcing and then into a response in the climate system is highly non-linear and poorly understood (Shindell et al., 2008; Fiore et al., 2012). Based on a synthesis of measured aerosol number concentrations and size distribution combined with boundary layer growth modelling Paasonen et al. (2013) estimated a growing-season indirect radiative cloud albedo feedback of -0.5 $Wm^{-2}K^{-1}$ for the Siberian larch region. The observation-based indirect feedback factors exceeded direct ones by roughly an order of magnitude (Paasonen et al., 2013), but a simple extrapolation based on the region's growing season temperature increases of *c.* 5.5 K simulated at the end of the 21st century in our study with the ECHAM GCM does not account for the important non-linearities in the system. Present-day CCN (1.0%) concentration over Siberia was estimated to vary from extremely low values of less than 50 cm^{-3} north of 60°N to a few hundred per cc in the southern part of Siberian domain (Figure 3). Over the larch-dominated area (Figure 1) the sensitivity of CCN to *E** was 5-10%. In order to put measurements and model simulations into context, simulated CCN concentrations (at the Spasskaya Pad location) were evaluated against observations during May-August, using particle diameter (dp) >100nm as proxy for CCN, since CCN at different supersaturations was unavailable in the observations. The model reproduces the observed May-August average CCN concentration (dp>100 nm) and CCN maximum location in July (not shown), but the seasonal variation was overestimated in the simulations. ECHAM-HAM indicates a transition from very clean spring aerosol population of ~100 cm^{-3} to high July concentrations ranging from 800 to 1200 cm^{-3} in the Yakutsk region. By contrast, observations show only moderate monthly CCN variability from 550 cm^{-3} in May to 750 cm^{-3} in July. While the simulated low spring concentrations likely reflect unaccounted-for anthropogenic emissions, the simulated high summer concentrations result from strong wildfire emissions in the region in the applied emission inventory (see below).

Whether or not BVOCs can increase the availability of ~~cloud condensation nuclei (CCN)~~CCN depends on the availability of sub-CCN sized particles (O'Donnell et al., 2011). In the future, a scenario of decreasing anthropogenic emissions led to a strong decrease in calculated atmospheric SO_2 concentrations and also of particle nucleation (Makkonen et al., 2012a). In the model experiments ~~A~~anthropogenic primary emissions are introduced ~~to the model~~ as 60 nm particles, hence condensation of sulfuric acid and organic vapours is generally needed in order to grow these particles to CCN sizes. ~~In Siberia, t~~ However, the modelled primary particle emissions are dominated by wildfires, which are assumed to inject large particles with 150 nm diameter. ~~What is more,~~ SOA formation only partly enhances the survival of small particles by providing additional growth (Makkonen et al., 2012a), but partly also suppresses it by increasing the coagulation sink for small particles (Figure A2, lower left panel; see also O'Donnell et al., 2011).

The assumption of unchanging oxidant fields induces some uncertainty for future simulations and inconsistency with present-day simulations with varying biogenic emissions, since both anthropogenic and biogenic emissions are likely to modify the atmospheric oxidative capacity. Nudging towards reanalysis meteorology establishes evaluation of BVOC-aerosol coupling with unchanged meteorological fields, but restricts the model in terms of aerosol-climate feedbacks, since e.g., nudging future climate simulations with present-day meteorological winds is based on the assumption that e.g. ~~cloudiness,~~ or wind direction and –speed etc. are not changing.

When only BVOC emissions were changed between present day and levels simulated for climate in 2100, the relatively higher emission of BVOC ~~under ambient and future conditions~~ leads to substantially increased aerosol growth rates (GR) over a large part of the Siberian domain. This was the case even though we chose the conservative estimate based on the low measured E^* of 1.9 μg C m^{-2} h^{-1}. However, GR is not the only factor determining levels of CCN. I~~i~~ncreased aerosol mass due to increased SOA formation led also to an increase in the condensation sink and eventually to even decreased particle formation rates in some regions (Figure A2, lower right panel). These competing effects of increased growth and increased sink are essential for quantifying the importance of the cloud albedo forcing feedback. ~~In addition, the negative effect~~We can also show that the patterns of changes in CCN ~~via~~ in response to future BVOC emissions are additionally ~~may also be altered through~~affected by changes in the aerosol background ~~(e.g., fire)~~, which strongly influences the indirect aerosol effect of SOA. ~~, since i~~In large parts of Siberia, the simulated BVOC oxidation products condense on CCN-sized aerosols already present from wildfires. ~~In the applied future scenarios, Siberian wildfire intensity was assumed to increase (Makkonen et al., 2012a).~~ When simulation results were separated ~~for~~ into ~~areas~~ regions of low and high wildfire emissions (Figure 4) ~~it becomes clear that in~~ areas of low wildfire activity had ~~, the~~ relatively large increase in SOA formation ~~was proportionally high~~ (60%) in nucleation mode (d_p<10 nm). ~~, and t~~The relative increases in SOA formation in Aitken, accumulation and coarse modes were 50%, 31% and 40%, respectively. However, the distribution of BVOC oxidation products was rather different in areas of high wildfire activity: the condensation of SOA depends on surface area and organic mass of the population, both of which are shifted towards larger modes in wildfire-intensive areas. SOA formation in coarse mode was more than doubled, while SOA in nucleation mode decreased by 30% due to decrease in nucleation rates and increase in vapour sink in large aerosol modes. ~~However, the distribution of BVOC~~

~~oxidation products was rather different in areas of high wildfire activity. SOA formation in coarse mode was more than doubled, while SOA in nucleation mode decreased by 30%.~~ It is clear that the effect of increased BVOC emission on particle population has distinct effects depending on existing background aerosol distribution. Moreover, CCN at 1.0% supersaturation was used, even though "realistic" supersaturations are generally lower. The CCN(1.0%) concentration therefore provide a upper limit for CCN concentration. In the aerosol model, neither the simulated CCN(1.0%) nor e.g., CCN(0.2%) correspond clearly to either Aitken or accumulation modes. CCN at 0.2% would reflect larger aerosols, and hence the changes in CCN(0.2%) would be less sensitive to aerosol and precursor sources (see corresponding Figure A3).

Averaged over Siberian areas of low wildfire activity, the median (mean) increase of CCN(0.2%) was calculated to be 1% (7%) due to BVOC emissions changes from ~~year 2000 to year 2100~~present-day levels to the end of the 21st century, while areas of high wildfire emission lead to median (mean) increase of 0.3% (0.5%).

Even though the Siberian *MT* emissions more than double until 2100 (~~Table 1~~Table 2), the increasing wildfire emissions and decreasing new particle formation due to reductions in anthropogenic SO_2 largely offset the effect of increased BVOC emissions on CCN concentration. In wildfire plumes, the simulated CCN concentrations were high even without BVOC-induced growth of smaller particles. The radiative effect due to BVOC emission change between ~~years~~ *ca.* 2000 and *ca.* 2100 was estimated from ECHAM-HAM simulations averaged over 5 years. The increase in BVOC emission leading to additional secondary organic aerosol induces a -0.2 W m^{-2} change in direct clear-sky aerosol forcing over the Siberian domain ~~until the year 2100~~at the end of the 21st century. Furthermore, the increase in CCN concentrations leads to a strengthening of the cloud radiative effect by -0.5 W m^{-2} (~~Table 2~~Table 3). These changes in radiative fluxes only take into account the changing BVOC emission, and the potential concurrent changes in anthropogenic and wildfire emissions might decrease the simulated radiative effect of biogenic SOA (Carslaw et al., 2013).

5. Implications, limitations and future progress

Up to now, studies that investigate the role of terrestrial vegetation dynamics and carbon cycle in the climate system typically account solely for CO_2, while studies that look at BVOC-climate interactions often ignore other processes, especially interactions with vegetation dynamics or the CO_2- balance of ecosystems. However, for understanding the full range of interactions between atmospheric composition, climate change and terrestrial processes we need a much more integrative perspective. Our analysis seeks to provide an example of how to quantify a number of climatically relevant ecosystem processes in the large Eastern Siberian region in a consistent observational and modelling framework that accounts for the multiple interactions between emissions, vegetation and soils. It poses a challenge to combine effects of well mixed greenhouse gases and locally constrained, short-lived substances. On global-scale level, the opposing estimates in radiative effects from ecosystem-CO_2 and -BVOC-SOA interactions are miniscule but it is to be expected that some of the forcing effects from SOA could lead to a notable change in regional temperatures. Clearly, our numbers are uncertain but they pinpoint the necessity for assessing surface-atmosphere exchange processes comprehensively in climate feedback analyses. While doing so, we are aware of the fact that a number of additional processes are not included in our analysis. For instance, it remains to be investigated whether a

similar picture would emerge when additional feedback mechanisms are taken into consideration, e.g. SOA formation from isoprene (Henze and Seinfeld, 2006) or effects of atmospheric water vapour on reaction rates and aerosol loads, or that some of the SOA might like to partition more to the gas-phase in a warmer climate. Likewise, neither the albedo effect of northwards migrating vegetation (Betts, 2000; Zhang et al., 2014), changes in the hydrology (which affects CH_4 and N_2O vs. CO_2 fluxes), nor changes in C-N interactions (Zaehle et al., 2010) are considered here, which would require a coupled ESM that combines a broad range of dynamically varying ecosystem processes with full treatment of air chemistry and aerosol interactions. Quantifying the full range of terrestrial climate feedbacks, either globally or regionally, with consistent model frameworks that account for the manifold interactions is not yet possible with today's modelling tools.

Acknowledgements

AA acknowledges support from Swedish Research Council VR, and the Helmholtz Association ATMO Programme, and its Initiative and Networking Fund. The study was also supported by the Finnish Academy, grant 132100. The EU FP7 Bacchus project (grant agreement 603445) is acknowledged for financial support. PM acknowledges support from the VR Linnaeus Centre of Excellence LUCCI, RM Makkonen acknowledges support from the Nordic Centre of Excellence CRAICC. This study is a contribution to the Strategic Research Area MERGE.

References

Ahlström, A., Schurgers, G., Arneth, A., and Smith, B.: Robustness and uncertainty in terrestrial ecosystem carbon response to cmip5 climate change projections, Environmental Research Letters, 7, 044008, doi: 10.1088/1748-9326/7/4/044008 2012.

Arneth, A., Miller, P. A., Scholze, M., Hickler, T., Schurgers, G., Smith, B., and Prentice, I. C.: CO_2 inhibition of global terrestrial isoprene emissions: Potential implications for atmospheric chemistry, Geophysical Research Letters, 34, L18813, doi: 10.1029/2007GL030615, 2007a.

Arneth, A., Niinemets, U., Pressley, S., Back, J., Hari, P., Karl, T., Noe, S., Prentice, I. C., Serca, D., Hickler, T., Wolf, A., and Smith, B.: Process-based estimates of terrestrial ecosystem isoprene emissions: incorporating the effects of a direct CO_2-isoprene interaction, Atmospheric Chemistry and Physics, 7, 31-53, 2007b.

Arneth, A., Schurgers, G., Hickler, T., and Miller, P. A.: Effects of species composition, land surface cover, CO_2 concentration and climate on isoprene emissions from European forests, Plant Biol., 10, 150-162, doi:10.1055/s-2007-965247, 2008.

Arneth, A., Harrison, S. P., Zaehle, S., Tsigaridis, K., Menon, S., Bartlein, P. J., Feichter, J., Korhola, A., Kulmala, M., O'Donnell, D., Schurgers, G., Sorvari, S., and Vesala, T.: Terrestrial biogeochemical feedbacks in the climate system, Nature Geosci, 3, 525-532, doi: 10.1038/ngeo1905, 2010.

Arneth, A., Schurgers, G., Lathiere, J., Duhl, T., Beerling, D. J., Hewitt, C. N., Martin, M., and Guenther, A.: Global terrestrial isoprene emission models: sensitivity to variability in climate and vegetation, Atmos. Chem. Phys., 11, 8037-8052, 10.5194/acp-11-8037-2011, 2011.

Arneth, A., Mercado, L., Kattge, J., and Booth, B. B. B.: Future challenges of representing land-processes in studies on land-atmosphere interactions, Biogeosciences, 9, 3587-3599, 10.5194/bg-9-3587-2012, 2012.

Betts, R. A.: Offset of the potential carbon sink from boreal forestation by decreases in surface albedo, Nature, 408, 187-190, 2000.Bäck, J., Aalto, J., Henriksson, M., Hakola, H., He, Q., and Boy, M.:

598 Chemodiversity of a scots pine stand and implications for terpene air concentrations, Biogeosciences, 9,
599 689-702, 10.5194/bg-9-689-2012, 2012.
600 Carslaw, K. S., Boucher, O., Spracklen, D. V., Mann, G. W., Rae, J. G. L., Woodward, S., and Kulmala,
601 M.: A review of natural aerosol interactions and feedbacks within the earth system, Atmospheric Chemistry
602 and Physics, 10, 1701-1737, 2010.
603 Carslaw, K. S., Lee, L. A., Reddington, C. L., Pringle, K. J., Rap, A., Forster, P. M., Mann, G. W.,
604 Spracklen, D. V., Woodhouse, M. T., Regayre, L. A., and Pierce, J. R.: Large contribution of natural aerosols
605 to uncertainty in indirect forcing, Nature, 503, 67-71, 10.1038/nature12674, 2013.
606 Dentener, F., Kinne, S., Bond, T., Boucher, O., Cofala, J., Generoso, S., Ginoux, P., Gong, S.,
607 Hoelzemann, J. J., Ito, A., Marelli, L., Penner, J. E., Putaud, J. P., Textor, C., Schulz, M., van der Werf, G.
608 R., and Wilson, J.: Emissions of primary aerosol and precursor gases in the years 2000 and 1750 prescribed
609 data-sets for AeroCom, Atmos. Chem. Phys., 6, 4321-4344, 2006.
610 Dolman, A. J., Maximov, T. C., Moors, E. J., Maximov, A. P., Elbers, J. A., Kononov, A. V., Waterloo,
611 M. J., and van der Molen, M. K.: Net ecosystem exchange of carbon dioxide and water of far eastern
612 Siberian Larch (Larix cajanderii) on permafrost, Biogeosciences, 1, 133-146, 2004.
613 Ehn, M., Thornton, J. A., Kleist, E., Sipila, M., Junninen, H., Pullinen, I., Springer, M., Rubach, F.,
614 Tillmann, R., Lee, B., Lopez-Hilfiker, F., Andres, S., Acir, I. H., Rissanen, M., Jokinen, T., Schobesberger,
615 S., Kangasluoma, J., Kontkanen, J., Nieminen, T., Kurten, T., Nielsen, L. B., Jorgensen, S., Kjaergaard, H.
616 G., Canagaratna, M., Dal Maso, M., Berndt, T., Petaja, T., Wahner, A., Kerminen, V. M., Kulmala, M.,
617 Worsnop, D. R., Wildt, J., and Mentel, T. F.: A large source of low-volatility secondary organic aerosol,
618 Nature, 506, 476-479, doi: 10.1038/nature13032, 2014.
619 Elmendorf, S. C., Henry, G. H. R., Hollister, R. D., Bjork, R. G., Boulanger-Lapointe, N., Cooper, E. J.,
620 Cornelissen, J. H. C., Day, T. A., Dorrepaal, E., Elumeeva, T. G., Gill, M., Gould, W. A., Harte, J., Hik, D.
621 S., Hofgaard, A., Johnson, D. R., Johnstone, J. F., Jonsdottir, I. S., Jorgenson, J. C., Klanderud, K., Klein, J.
622 A., Koh, S., Kudo, G., Lara, M., Levesque, E., Magnusson, B., May, J. L., Mercado-Diaz, J. A., Michelsen,
623 A., Molau, U., Myers-Smith, I. H., Oberbauer, S. F., Onipchenko, V. G., Rixen, C., Schmidt, N. M., Shaver,
624 G. R., Spasojevic, M. J., Porhallsdottir, P. E., Tolvanen, A., Troxler, T., Tweedie, C. E., Villareal, S.,
625 Wahren, C. H., Walker, X., Webber, P. J., Welker, J. M., and Wipf, S.: Plot-scale evidence of tundra
626 vegetation change and links to recent summer warming, Nat. Clim. Chang., 2, 453-457, doi:
627 10.1038/nclimate1465, 2012.
628 Fisher, R., McDowell, N., Purves, D., Moorcroft, P., Sitch, S., Cox, P., Huntingford, C., Meir, P., and
629 Woodward, F. I.: Assessing uncertainties in a second-generation dynamic vegetation model caused by
630 ecological scale limitations, New Phytologist, 187, 666-681, 10.1111/j.1469-8137.2010.03340.x, 2010
631 Fiore, A. M., Naik, V., Spracklen, D. V., Steiner, A., Unger, N., Prather, M., Bergmann, D., Cameron-
632 Smith, P. J., Cionni, I., Collins, W. J., Dalsoren, S., Eyring, V., Folberth, G. A., Ginoux, P., Horowitz, L. W.,
633 Josse, B., Lamarque, J.-F., MacKenzie, I. A., Nagashima, T., O'Connor, F. M., Righi, M., Rumbold, S. T.,
634 Shindell, D. T., Skeie, R. B., Sudo, K., Szopa, S., Takemura, T., and Zeng, G.: Global air quality and
635 climate, Chemical Society Reviews, 41, 6663-6683, doi: 10.1039/c2cs35095e, 2012.
636 Guenther, A., Hewitt, C. N., Erickson, D., Fall, R., Geron, C., Graedel, T., Harley, P., Klinger, L., Lerdau,
637 M., McKay, W. A., Pierce, T., Scholes, B., Steinbrecher, R., Tallamraju, R., Taylor, J., and Zimmermann, P.:
638 A global model of natural volatile organic compound emissions, Journal of Geophysical Research, 100,
639 8873-8892, 1995.
640 Haapanala, S., Ekberg, A., Hakola, H., Tarvainen, V., Rinne, J., Hellen, H., and Arneth, A.: Mountain
641 birch - potentially large source of sesquiterpenes into high latitude atmosphere, Biogeosciences, 6, 2709-
642 2718, 2009.
643 Hallquist, M., Wenger, J. C., Baltensperger, U., Rudich, Y., Simpson, D., Claeys, M., Dommen, J.,
644 Donahue, N. M., George, C., Goldstein, A. H., Hamilton, J. F., Herrmann, H., Hoffmann, T., Iinuma, Y.,
645 Jang, M., Jenkin, M. E., Jimenez, J. L., Kiendler-Scharr, A., Maenhaut, W., McFiggans, G., Mentel, T. F.,
646 Monod, A., Seinfeld, J. H., Surratt, J. D., Szmigielski, R., and Wildt, J.: The formation, properties and
647 impact of secondary organic aerosol: Current and emerging issues, Atmos. Chem. Phys., 9, 5155-5235, 2009.
648 Hakola, H., Tarvainen, V., Back, J., Ranta, H., Bonn, B., Rinne, J., and Kulmala, M.: Seasonal variation
649 of mono- and sesquiterpene emission rates of Scots pine, Biogeosciences, 3, 93-101, 2006.
650 Hens, K., Novelli, A., Martinez, M., Auld, J., Axinte, R., Bohn, B., Fischer, H., Keronen, P., Kubistin, D.,
651 Nölscher, A. C., Oswald, R., Paasonen, P., Petäjä, T., Regelin, E., Sander, R., Sinha, V., Sipilä, M.,

652 Taraborrelli, D., Tatum Ernest, C., Williams, J., Lelieveld, J., and Harder, H.: Observation and modelling of
653 HO_x radicals in a boreal forest, Atmos. Chem. Phys., 14, 8723-8747, doi:10.5194/acp-14-8723-2014, 2014.
654 Henze, D., and Seinfeld, J. H.: Global secondary organic aerosol from isoprene oxidation, Geophysical
655 Research Letters, 33, L09812, doi: 10.1029/2006GL025976, 2006.
656 Hickler, T., Vohland, K., Feehan, J., Miller, P. A., Smith, B., Costa, L., Giesecke, T., Fronzek, S., Carter,
657 T. R., Cramer, W., Kuhn, I., and Sykes, M. T.: Projecting the future distribution of European potential
658 natural vegetation zones with a generalized, tree species-based dynamic vegetation model, Global Ecology
659 and Biogeography, 21, 50-63, doi: 10.1111/j.1466-8238.2010.00613.x, 2012.
660 Holst, T., Arneth, A., Hayward, S., Ekberg, A., Mastepanov, M., Jackowicz-Korczynski, M., Friborg, T.,
661 and Crill, P. M.: Bvoc ecosystem flux measurements at a high latitude wetland site, Atmospheric Chemistry
662 and Physics, 10, 1617-1634, 2010.
663 Hussein, T., Dal Maso, M., Petäjä, T., Koponen, I. K., Paatero, P., Aalto, P. P., Hämeri, K., and Kulmala,
664 M.: Evaluation of an automatic algorithm for fitting the particle number size distributions Boreal
665 Environment Research, 10, 337-355, 2005.
666 IPCC: Climate Change 2007: The Physical Science Basis. Summary for Policymakers. Contribution of
667 Working Group I to the Fourth Assessment Report of the Intergovernmental Panel on Climate Change,
668 Cambridge University Press, Cambridge, 2007.
669 Jokinen, T., Berndt, T., Makkonen, T., Kerminen, V.-M., Junninen, H., Paasonen, P., Stratmann, F.,
670 Herrmann, H., Guenther, A., Worsnop, D. R., Kulmala, M., Ehn, M., and Sipilä, M.: Production of extremely
671 low-volatile organic compounds from biogenic emissions: Measured yields and atmospheric implications,
672 Proceedings of the National Academy of Sciences of the United States of America,
673 doi:10.1073/pnas.1423977112, 2015.
674 Kajos, M. K., Hakola, H., Holst, T., Nieminen, T., Tarvainen, V., Maximov, T., Petäjä, T., Arneth, A.,
675 and Rinne, J.: Terpenoid emissions from fully grown East Siberian *Larix cajanderi* trees, Biogeosciences,
676 10, 4705-4719, doi: 10.5194/bg-10-4705-2013, 2013.
677 Kharuk, V., Ranson, k., and Dvinskaya, M.: Evidence of Evergreen Conifer Invasion into Larch
678 Dominated Forests During Recent Decades in Central Siberia, Eurasian Journal of Forest Research, 10, 163-
679 171, 2007.
680 Khvorostyanov, D. V., Ciais, P., Krinner, G., and Zimov, S. A.: Vulnerability of east Siberia's frozen
681 carbon stores to future warming, Geophys. Res. Lett., 35, L10703, doi:10710.1029/2008GL033639, 2008.
682 Kobak, K. I., Turchinovich, I. Y., Kondrasheva, N. Y., Schulze, E. D., Schulze, W., Koch, H., and
683 Vygodskaya, N. N.: Vulnerability and adaptation of the larch forest in eastern Siberia to climate change,
684 Water, Air, & Soil Pollution, 92, 119-127, 1996.
685 Koven, C. D., Ringeval, B., Friedlingstein, P., Ciais, P., Cadule, P., Khvorostyanov, D., Krinner, G., and
686 Tarnocai, C.: Permafrost carbon-climate feedbacks accelerate global warming, Proceedings of the National
687 Academy of Sciences of the United States of America, 108, 14769-14774, doi: 10.1073/pnas.1103910108,
688 2011.
689 Kulmala, M., Dal Maso, M., Makela, J. M., Pirjola, L., Vakeva, M., Aalto, P., Miikkulainen, P., Hameri,
690 K., and O'Dowd, C. D.: On the formation, growth and composition of nucleation mode particles, Tellus Ser.
691 B-Chem. Phys. Meteorol., 53, 479-490, doi: 10.1034/j.1600-0889.2001.530411.x, 2001.
692 Kulmala, M., Petäjä, T., Mönkkönen, P., Koponen, I. K., Dal Maso, M., Aalto, P., Lehtinen, K. E. J., and
693 Kerminen, V. M.: On the growth of nucleation mode particles: source rates of condensable vapor in polluted
694 and clean environments, Atmospheric Chemistry and Physics, 4, 409-416, 2005.
695 Lappalainen, H. K., Sevanto, S., Back, J., Ruuskanen, T. M., Kolari, P., Taipale, R., Rinne, J., Kulmala,
696 M., and Hari, P.: Day-time concentrations of biogenic volatile organic compounds in a boreal forest canopy
697 and their relation to environmental and biological factors, Atmospheric Chemistry and Physics, 9, 5447-
698 5459, 2009.
699 Makkonen, R., Asmi, A., Kerminen, V. M., Boy, M., Arneth, A., Guenther, A., and Kulmala, M.: BVOC-
700 aerosol-climate interactions in the global aerosol-climate model ECHAM5.5-HAM2, Atmos. Chem. Phys.,
701 12, 10077-10096, 10.5194/acp-12-10077-2012, 2012a.
702 Makkonen, R., Asmi, A., Kerminen, V. M., Boy, M., Arneth, A., Hari, P., and Kulmala, M.: Air pollution
703 control and decreasing new particle formation lead to strong climate warming, Atmos. Chem. Phys., 12,
704 1515-1525, doi: 10.5195/acp-1515-2012, 2012b.

Miller, P. A., Giesecke, T. T. Hickler, R. H. W. Bradshaw, B. Smith, H. Seppä, P. J. Valdes, M. T. Sykes. Exploring climatic and biotic controls on Holocene vegetation change in Fennoscandia, Journal of Ecology 96(2), 247-259, 10.1111/j.1365-2745.2007.01342.x, 2008

Miller, P. A., and Smith, B.: Modelling tundra vegetation response to recent arctic warming, Ambio, 41, 281-291, doi: 10.1007/s13280-12-306-1, 2012.

Mitchell, T. D., and Jones, P. D.: An improved method of constructing a database of monthly climate observations and associated high-resolution grids, International Journal of Climatology, 25, 693-712, 2005.

Mochizuki, T., Tani, A., Takahashi, Y., Saigusa, N., Ueyama, M., 2014. Long-term measurement of terpenoid flux above a Larix kaempferi forest using a relaxed eddy accumulation method. Atmospheric Environment 83, 53-61.

Moser, L., Fonti, p., Büntgen, U., Esper, J., Luterbacher, J., Franzen, J., and Frank, D.: Timing and duration of European larch growing season along altitudinal gradients in the Swiss Alps, Tree Physiology, 30, 225-233. doi:10.1093/treephys/tpp108, 2012.

Nieminen, T., Lehtinen, K. E. J., and Kulmala, M.: Sub-10 nm particle growth by vapor condensation – effects of vapor molecule size and particle thermal speed, Atmos. Chem. Phys., 10, 9773-9779, doi: 10.5194/acp-10-9773-2010, 2010.

Nieminen, T., Asmi, A., Dal Maso, M., Aalto, P. P., Keronen, P., Petaja, T., Kulmala, M., and Kerminen, V.-M.: Trends in atmospheric new-particle formation: 16 years of observations in a boreal-forest environment, Boreal Environment Research, 19, 191-214, 2014.

Niinemets, U., Tenhunen, J. D., Harley, P. C., and Steinbrecher, R.: A model of isoprene emission based on energetic requirements for isoprene synthesis and leaf photosynthetic properties for *Liquidambar* and *Quercus*, Plant, Cell and Environment, 22, 1319-1335, 1999.

Niinemets, Ü., Monson, R. K., Arneth, A., Ciccioli, P., Kesselmeier, J., Kuhn, U., Noe, S. M., Penuelas, J., and Staudt, M.: The emission factor of volatile isoprenoids: caveats, model algorithms, response shapes and scaling, Biogeosciences, 7, 1809-1832, SRef-ID: 1726-4189/bg/2010-7-1809, 2010.

O'Donnell, D., Tsigaridis, K., and Feichter, J.: Estimating the direct and indirect effects of secondary organic aerosols using ECHAM5-HAM, Atmos. Chem. Phys., 11, 8635-8659, doi: 10.5194/acp-11-8635-2011, 2011.

Ohta, T., Hiyama, T., Tanaka, H., Kuwada, T., Maximov, T. C., Ohata, T., and Fukushima, Y.: Seasonal variation in the energy and water exchanges above and below a larch forest in eastern Siberia, Hydrological Processes, 15, 1459-1476, 2001.

Paasonen, P., Asmi, A., Petaja, T., Kajos, M. K., Aijala, M., Junninen, H., Holst, T., Abbatt, J. P. D., Arneth, A., Birmili, W., van der Gon, H. D., Hamed, A., Hoffer, A., Laakso, L., Laaksonen, A., Richard Leaitch, W., Plass-Dulmer, C., Pryor, S. C., Raisanen, P., Swietlicki, E., Wiedensohler, A., Worsnop, D. R., Kerminen, V.-M., and Kulmala, M.: Warming-induced increase in aerosol number concentration likely to moderate climate change, Nature Geosci, 6, 438-442, doi: 10.1038/ngeo1800, 2013.

Penuelas, J., and Staudt, M.: Bvocs and global change, Trends in Plant Science, 15, 133-144, 10.1016/j.tplants.2009.12.005, 2010.

Piao, S., Friedlingstein, P., Ciais, P., Zhou, L., and Chen, A.: Effect of climate and CO_2 changes on the greening of the Northern Hemisphere over the past two decades, Geophys. Res. Lett., 33, L23402, doi: 10.1029/2006gl028205, 2006.

Rantala, P., Aalto, J., Taipale, R., Ruuskanen, T.M., Rinne, J., 2015. Annual cycle of volatile organic compound exchange between a boreal pine forest and the atmosphere. Biogeosciences 12, 5753-5770.

Riahi, K., Gruebler, A., and Nakicenovic, N.: Scenarios of long-term socio-economic and environmental development under climate stabilization, Technol. Forecast. Soc. Change, 74, 887-935, 2007.

Rohrer, F. and Berresheim, H.: Strong correlation between levels of tropospheric hydroxyl radicals and solar ultraviolet radiation, Nature, 442, 184–187, 2006.

Romanovsky, V. E., Drozdov, D. S., Oberman, N. G., Malkova, G. V., Kholodov, A. L., Marchenko, S. S., Moskalenko, N. G., Sergeev, D. O., Ukraintseva, N. G., Abramov, A. A., Gilichinsky, D. A., and Vasiliev, A. A.: Thermal state of permafrost in russia, Permafrost and Periglacial Processes, 21, 136-155, 10.1002/ppp.683, 2010.Ruuskanen, T. M., Kajos, M. K., Hellén, H., Hakola, H., Tarvainen, V., and Rinne, J.: Volatile organic compound emissions from Siberian larch, Atmospheric Environment, 41, doi:10.1016/j.atmosenv.2007.05.036 2007.

758 Schaefer, K., Lantuit, H., Romanovsky, V. E., Schuur, E. A. G., and Witt, R.: The impact of the
759 permafrost carbon feedback on global climate, Environmental Research Letters, 9, 085003, 10.1088/1748-
760 9326/9/8/085003, 2014.
761 Schneider von Deimling, T., Meinshausen, M., Levermann, A., Huber, V., Frieler, K., Lawrence, D. M.,
762 and Brovkin, V.: Estimating the near-surface permafrost-carbon feedback on global warming,
763 Biogeosciences, 9, 649-665, doi: 10.5194/bg-9-649-2012, 2012.
764 Schurgers, G., Arneth, A., Holzinger, R., and Goldstein, A. H.: Process-based modelling of biogenic
765 monoterpene emissions: sensitivity to temperature and light, Atmospheric Chemistry and Physics, 9, 3409-
766 3423, 2009a.
767 Schurgers, G., Hickler, T., Miller, P. A., and Arneth, A.: European emissions of isoprene and
768 monoterpenes from the Last Glacial Maximum to present, Biogeosciences, 6, 2779-2797, 2009b.
769 Schuur, E. A. G., Vogel, J. G., Crummer, K. G., Lee, H., Sickman, J. O., and Osterkamp, T. E.: The effect
770 of permafrost thaw on old carbon release and net carbon exchange from tundra, Nature, 459, 556-559, doi:
771 10.1038/nature08031, 2009.
772 Serreze, M. C., Walsh, J. E., Chapin, F. S., Osterkamp, T., Dyurgerov, M., Romanovsky, V., Oechel, W.
773 C., Morison, J., Zhang , T., and Barry, R. G.: Observational evidence of recent change in the northern high-
774 latitude environment, Climatc Change, 46, 159-207, 2000.
775 Shindell, D. T., Levy, H., Schwarzkopf, M. D., Horowitz, L. W., Lamarque, J. F., and Faluvegi, G.:
776 Multimodel projections of climate change from short-lived emissions due to human activities, Journal of
777 Geophysical Research-Atmospheres, 113, doi:10.1029/2007JD009152, D11109, 2008.
778 Shuman, J. K., Tchebakova, N. M., Parfenova, E. I., Soja, A. J., Shugart, H. H., Ershov, D., and
779 Holcomb, K.: Forest forecasting with vegetation models across russia, Canadian Journal of Forest Research,
780 45, 175-184, 10.1139/cjfr-2014-0138, 2015
781 Sistla, S. A., Moore, J. C., Simpson, R. T., Gough, L., Shaver, G. R., and Schimel, J. P.: Long-term
782 warming restructures Arctic tundra without changing net soil carbon storage, Nature, 497, 615-618, doi:
783 10.1038/nature12129, 2013.
784 Sitch, S., Smith, B., Prentice, I. C., Arneth, A., Bondeau, A., Cramer, W., Kaplan, J. O., Levis, S., Lucht,
785 W., Sykes, M. T., Thonicke, K., and Venevsky, S.: Evaluation of ecosystem dynamics, plant geography and
786 terrestrial carbon cycling in the LPJ dynamic global vegetation model, Glob. Change Biol., 9, 161-185, 2003.
787 Sitch, S., Cox, P. M., Collins, W. J., and Huntingford, C.: Indirect radiative forcing of climate change
788 through ozone effects on the land-carbon sink, Nature, 448 (7155), 791-794, doi:10.1038/nature06059, 2007.
789 Smith, B., Prentice, I. C., and Sykes, M. T.: Representation of vegetation dynamics in the modelling of
790 terrestrial ecosystems: comparing two contrasting approaches within European climate space, Global
791 Ecology & Biogeography, 10, 621-637, 2001.
792 Soja, A. J., Tchebakova, N. M., French, N. H. F., Flannigan, M. D., Shugart, H. H., Stocks, B. J.,
793 Sukhinin, A. I., Parfenova, E. I., Chapin Iii, F. S., and Stackhouse, J. P. W.: Climate-induced boreal forest
794 change: Predictions versus current observations, Global and Planetary Change, 56, 274-296, doi:
795 10.1016/j.gloplacha.2006.07.028, 2007.
796 Spracklen, D. V., Bonn, B., and Carslaw, K.: Boreal forests, aerosols and the impacts on clouds and
797 climate, Philosophical Transactions of the Royal Society of London Series A, 366, 4613–4626, doi:
798 10.1098/rsta.2008.0201, 2008a.
799 Spracklen, D. V., Carslaw, K. S., Kulmala, M., Kerminen, V.-M., Sihto, S.-L., Riipinen, I., Merikanto, J.,
800 Mann, G. W., Chipperfield, M. P., Wiedensohler, A., Birmili, W., and Lihavainen, H.: Contribution of
801 particle formation to global cloud condensation nuclei concentrations, Geophysical Research Letters, 35,
802 L06808, doi: 10.01029/2007GL033038, 2008b.Staudt, M., Mandl, N., Joffre, R., and Rambal, S.:
803 Intraspecific variability of monoterpene composition emitted by quercus ilex leaves, Canadian Journal of
804 Forest Research, 31, 174-180, 10.1139/x00-153, 2001.
805 Staudt, M., Joffre, R., and Rambal, S.: How growth conditions affect the capacity of *quercus ilex* leaves
806 to emit monoterpenes, New Phytologist, 158, 61-73, 2003.
807 Stier, P., Feichter, J., Kinne, S., Kloster, S., Vignati, E., Wilson, J., Ganzeveld, L., Tegen, I., Werner, M.,
808 Balkanski, Y., Schulz, M., and Bouche, O.: The aerosol-climate model Echam5-Ham, Atmospheric
809 Chemistry and Physics, 5, 11125-11156, 2005.

Svenningsson, B., Arneth, A., Hayward, S., Holst, T., Massling, A., Swietlicki, E., Hirsikko, A., Junninen, H., Riipinen, I., Vana, M., dal Maso, M., Hussein, T., and Kulmala, A. E.: Aerosol particle formation events and analysis of high growth rates observed above a subarctic wetland–forest mosaic, Tellus B, 58, 353-364, doi: 10.1111/j.1600-0889.2008.00351.x, 2008.

Takeshi, O., Maximov, T. C., Dolman, A. J., Nakai, T., van der Molen, M. K., Kononov, A. V., Maximov, A. P., Hiyama, T., Iijima, Y., Moors, E. J., Tanaka, H., Toba, T., and Yabuki, H..: Interannual variation of water balance and summer evapotranspiration in an eastern Siberian larch forest over a 7-year period (1998–2006), Agricultural and Forest Meteorology, 48, 1940-1953, 2008.

Tarnocai, C., Canadell, J. G., Schuur, E. A. G., Kuhry, P., Mazhitova, G., and Zimov, S.: Soil organic carbon pools in the northern circumpolar permafrost region, Global Biogeochemical Cycles, 23, Gb2023, doi: 10.1029/2008gb003327, 2009.

Tchebakova, N. M., Rehfeldt, G. E., and Parfenova, E. I.: Impacts of climate change on the distribution of *Larix spp.* and *Pinus sylvestris* and their climatypes in Siberia, Mitigation and Adaptation Strategies for Global Change, 11, 861-882, doi: 10.1007/s11027-005-9019-0, 2006.

Thonicke, K., Venevsky, S., Sitch, S., and Cramer, W.: The role of fire disturbance for global vegetation dynamics. Coupling fire into a Dynamic Global Vegetation Model, Global Ecology & Biogeography, 10, 661-678, 2001.

Tunved, P., Hansson, H. C., Kerminen, V. M., Strom, J., Maso, M. D., Lihavainen, H., Viisanen, Y., Aalto, P. P., Komppula, M., and Kulmala, M.: High natural aerosol loading over boreal forests, Science, 312, 261-263, doi: 10.1126/science.1123052, 2006.

Tsigaridis, K., Daskalakis, N., Kanakidou, M., Adams, P. J., Artaxo, P., Bahadur, R., Balkanski, Y., Bauer, S. E., Bellouin, N., Benedetti, A., Bergman, T., Berntsen, T. K., Beukes, J. P., Bian, H., Carslaw, K. S., Chin, M., Curci, G., Diehl, T., Easter, R. C., Ghan, S. J., Gong, S. L., Hodzic, A., Hoyle, C. R., Iversen, T., Jathar, S., Jimenez, J. L., Kaiser, J. W., Kirkevåg, A., Koch, D., Kokkola, H., Lee, Y. H, Lin, G., Liu, X., Luo, G., Ma, X., Mann, G. W., Mihalopoulos, N., Morcrette, J.-J., Müller, J.-F., Myhre, G., Myriokefalitakis, S., Ng, N. L., O'Donnell, D., Penner, J. E., Pozzoli, L., Pringle, K. J., Russell, L. M., Schulz, M., Sciare, J., Seland, Ø., Shindell, D. T., Sillman, S., Skeie, R. B., Spracklen, D., Stavrakou, T., Steenrod, S. D., Takemura, T., Tiitta, P., Tilmes, S., Tost, H., van Noije, T., van Zyl, P. G., von Salzen, K., Yu, F., Wang, Z., Wang, Z., Zaveri, R. A., Zhang, H., Zhang, K., Zhang, Q., and Zhang, X.: The AeroCom evaluation and intercomparison of organic aerosol in global models, Atmos. Chem. Phys., 14, 10845-10895, doi:10.5194/acp-14-10845-2014, 2014.

Vignati, E., Wilson, J., and Stier, P.: M7: An efficient size-resolved aerosol microphysics module for large-scale aerosol transport models, Journal of Geophysical Research, 109, D22202, doi:10.1029/2003JD004485, 2004.

Wagner, V.: Analysis of a Russian landscape map and landscape classification for use in computer-aided forestry research, International Institute for Applied Systems Analysis, Laxenburg, 1997.

Wania, R., Ross, I., and Prentice, I. C.: Integrating peatlands and permafrost into a dynamic global vegetation model: I. Evaluation and sensitivity of physical land surface processes, Global Biogeochemical Cycles 23, GB3014, doi:10.1029/2008GB003412, 2009.

Zhang, K., O'Donnell, D., Kazil, J., Stier, P., Kinne, S., Lohmann, U., Ferrachat, S., Croft, B., Quaas, J., Wan, H., Rast, S., and Feichter, J.: The global aerosol-climate model ECHAM-HAM, version 2: sensitivity to improvements in process representations, Atmospheric Chemistry and Physics, 12, 8911–8949, doi:10.5194/acp-8912-8911-2012, 2012.

Zhang, W., Jansson, C., Miller, P. A., Smith, B., and Samuelsson, P.: Biogeophysical feedbacks enhance the arctic terrestrial carbon sink in regional earth system dynamics, Biogeosciences, 11, 5503-5519, 10.5194/bg-11-5503-2014, 2014.

Zhang, K., Wan, H., Liu, X., Ghan, S. J., Kooperman, G. J., Ma, P.-L., Rasch, P. J., Neubauer, D., and Lohmann, U.: Technical note: On the use of nudging for aerosol–climate model intercomparison studies, Atmos. Chem. Phys., 14, 8631-8645, doi:10.5194/acp-14-8631-2014, 2014.

Zaehle, S., Friedlingstein, P., and Friend, A. D.: Terrestrial nitrogen feedbacks may accelerate future climate change, Geophysical Research Letters, 37, L01401, doi: 10.01029/02009GL041345 2010.

863 Table 1: Overview over modelled processes, and model-specific features. For further details see text.

Process	Model	Input	Input source	Resolution	Configuration	Specific features
BVOC emissions	LPJ-GUESS, dynamic global vegetation model	Air temperature, precipitation, short-wave radiation (monthly, interpolated to daily), atmospheric CO2 levels (annual).	ECHAM historical (20th century) and RCP 8.5 (21st century), interpolated to CRU climate, following Ahlström et al. (2012)	0.5 X 0.5 degrees horizontal	As in Arneth et al. (2007a) and Schurgerst et al. (2009b)	BNS plant functional type adopted for larch-specific parameters (see text). Inhibition of BVOC emissions by atmospheric CO_2 can be switched on and off.
Ecosystem dynamics and carbon cycle	As above	As above	As above	As above	As in Miller and Smith, 2012	Including permafrost module
Aerosol number concentration and size distribution: black carbon, organic carbon, dust, sea salt and sulfate	ECHAM5.5-HAM2, Global climate model coupled with aerosol microphysics	Emissions of BVOC, from wildfire, anthropogenic sources, dust and seasalt	Climate generated as part of simulation nudged to ERA-40; BVOC from LPJ-GUESS; as in Makkonen et al., (2012); dust/seasalt modelled interactively, anthropogenic and wildfire emissions fixed to present day (Stier et al., 2005; Makkonen et al., (2012)	T63 spectral resolution, 31 vertical hybrid sigma levels	As in Makkonen et al. (2012)	SOA module includes formation of extremely low volatility organic compounds from MT oxidation (Jokinen et al. 2015)
Total particle and cloud concentration nuclei concentration, radiative effects	As above	As above	As above	As above	As in Lohmann et al., 2007	Aerosol concentrations are interactively coupled to the cloud-microphysics scheme, calculation of aerosol direct and indirect effect

864

~~Table 1~~Table 2: **Simulated changes in net primary productivity, BVOC emissions, and C pool size in vegetation and soils.** Unless stated otherwise, values are for the simulated Siberian domain (76-164°E, 46-71°N), and represent an area of 1.2 E^7 km^2. NPP_{global} (given as a reference value) is global vegetation net primary productivity (Pg C a^{-1}). BVOC in Tg C a^{-1}, CO_2-C fluxes in Pg C a^{-1}, C pools in PgC.

Simulations for monoterpene emissions for the boreal needleleaf summergreen (BNS) plant functional type compared three cases (indicated as different subscripts for "Total_MT_{BNS}"): ~~were made~~ using maximum (9.6 µgC g^{-1} h^{-1}) and minimum (1.9 µgC~~µgC~~ g^{-1} h^{-1}) values for *E** measured in Spasskaya Pad (see text), and *E** = 6.2µgC~~µgC~~ g^{-1} h^{-1} ~~represents~~ as a weighted average from all observations at the Spasskaya Pad location. For BVOC, CO_2 inhibition was switched on and off (Arneth et al., 2007b).

	1981-2000	2031-2050	2081-2100
NPP_{global}	58 ± 15	66 ± 17	76 ± 14
NPP	3.5 ± 0.2	4.5 ± 0.2	5.9 ± 0.2
Carbon in circumpolar permafrost region:			
Vegetation	109 ± 0.7	106 ± 1.6	78 ± 1.8
Litter	81 ± 0.5	68 ± 0.3	44 ± 0.3
Soil (0 to 2 m depth)	454 ±0.03	392 ± 0.4	255 ± 0.5
Total	644 ± 0.4	567 ± 1.1	377 ± 1.0
C-pools in permafrost area of study domain			
Vegetation	41 ± 0.6	38 ± 0.6	35 ± 0.7
Litter	40 ± 0.3	34 ± 0.2	23 ± 0.2
Soil (0 to 2 m depth)	216 ± 0.06	187 ± 0.1	140 ± 0.3
Total	297 ± 0.4	259 ± 0.4	198 ± 0.2
C-pools in entire Siberian study domain:			
Vegetation	45 ± 0.5	56 ± 1.5	77 ± 2.8
Litter	41 ± 0.5	43 ± 0.3	41 ± 0.7
Soil (0 to 2 m depth)	219 ± 0.3	221 ± 0.3	223 ± 0.3
Total	305 ± 1.1	320 ± 2.1	342 ± 2.0
BVOC, with CO_2 inhibition:			
Total_iso	4.11 ± 0.29	4.52 ± 0.32	4.80 ± 0.24
BNE, MT	1.03 ± 0.07	1.06 ± 0.06	1.02 ± 0.04
BINE, MT	0.23 ± 0.01	0.23 ± 0.01	0.18 ± 0.01
BNS, MT_1.9	0.09 ± 0.01	0.10 ± 0.02	0.09 ± 0.01
BNS, MT_6.2	0.28 ± 0.04	0.33 ± 0.06	0.29 ± 0.04
BNS, MT_9.6	0.43 ± 0.06	0.52 ± 0.09	0.45 ± 0.06
Total_$MT_{BNS_1.9}$	1.40 ± 0.09	1.44 ± 0.10	1.33 ± 0.06
Total_ $MT_{BNS\_6.2}$	1.60 ± 0.11	1.68 ± 0.14	1.53 ± 0.88
Total_ $MT_{BNS\ \_9.6}$	1.75 ± 0.12	1.86 ± 0.16	1.69 ± 0.10
BVOC, no CO_2 inhibition:			
Total_iso	3.9 ± 0.29	6.0 ± 0.48	11.0 ± 1.06
BNE, MT	0.99 ± 0.07	1.41 ± 0.1	2.33 ± 0.19
BINE, MT	0.22 ± 0.01	0.30 ± 0.02	0.42 ± 0.02
BNS, MT_1.9	0.08 ± 0.01	0.14 ± 0.02	0.20 ± 0.03
BNS, MT_6.2	0.21±0.03	0.35±0.06	0.52±0.07
BNS, MT_9.6	0.42±0.06	0.69±0.11	1.02±0.13

Total_$MT_{BNS_1.9}$	1.34±0.09	1.92±0.13	3.04±0.23
Total_ $MT_{BNS\_6.2}$	1.47±0.10	2.13±0.16	3.36±0.27
Total_ $MT_{BNS\_9.6}$	1.67±0.13	2.47±0.22	4.90±0.47

Abbreviations:
NPP: net primary productivity;
BNE: boreal needleleaf evergreen PFT, shade tolerant;
BINE: boreal needleleaf evergreen PFT, intermediate shade-tolerant;
BNS: boreal needleleaf summergreen PFT ("larch"), shade intolerant, continentality index as in Sitch et al., (2003);
Iso: isoprene;
MT, monoterpenes.

~~Table 2~~Table 3: Simulated changes in radiative effects due to change in BVOC emission between years 2000 and 2100, averaged over Siberian domain, Northern Hemisphere and globally. CRF: cloud radiative forcing; CSDRF, direct aerosol effect that accounts only for clear-sky short-wave forcing.

	ΔCRF (Wm^{-2})	ΔCSDRF (Wm^{-2})
Siberia	-0.50	-0.21
Northern hemisphere	-0.30	-0.01
Global	-0.03	-0.01

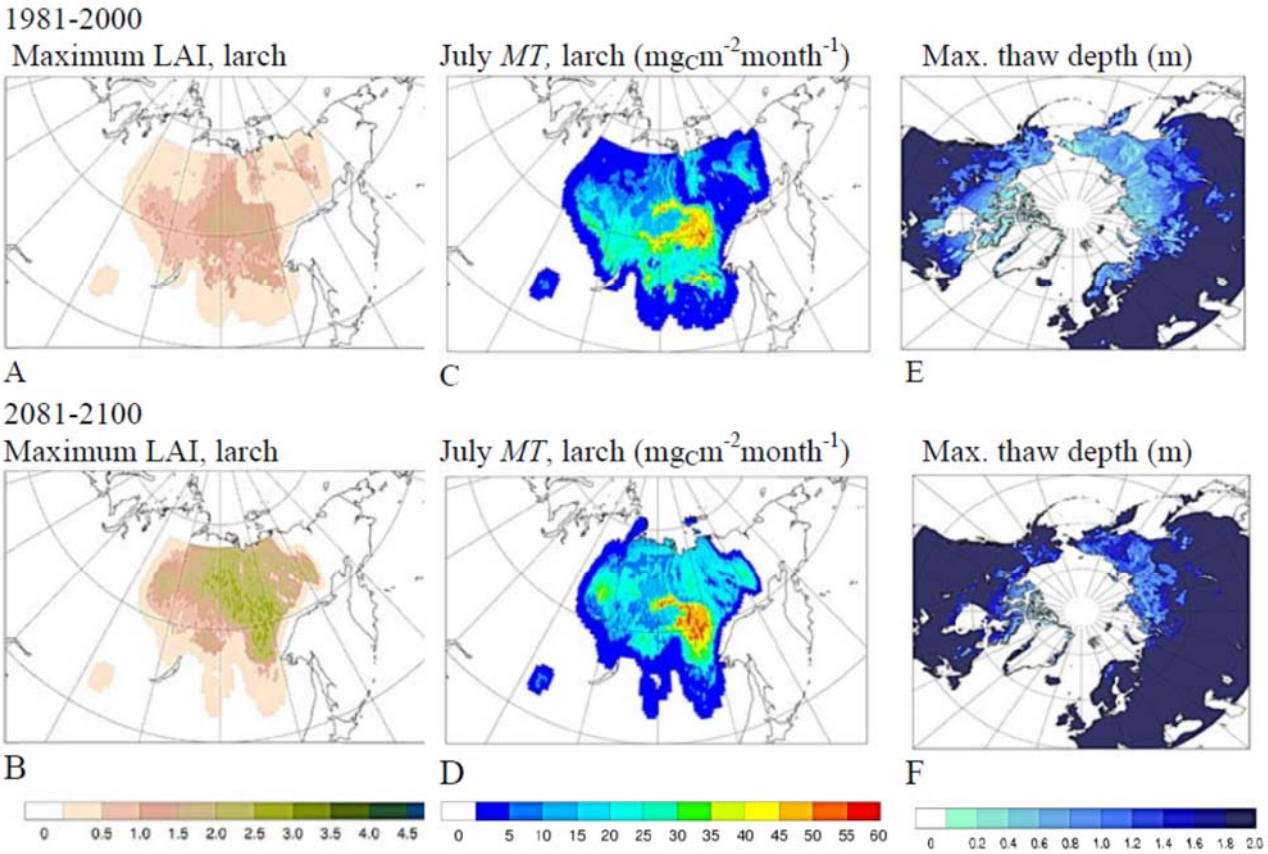

Figure 1: Simulated maximum summer monthly leaf area index (LAI; A, B) and July emissions of monoterpenes (C, D; mgC m^{-2} $month^{-1}$) from Eastern Siberian larch. The latter were calculated applying emission factors of 6.2**,** obtained from the measurements at Spasskaya Pad. Panels E and F: maximum permafrost thaw depth (August), shown here as the circumpolar map for comparison with Tarnocai et al. (Tarnocai et al., 2009). Values are averages for a simulation 1981-2000 (panels A, C, E), and for 2081-2100 (panels B, D, F), applying climate and CO_2 concentrations from ECHAM-RCP8.5. Emissions in panel C, D do not account for direct CO_2 inhibition (see also Figure A1).

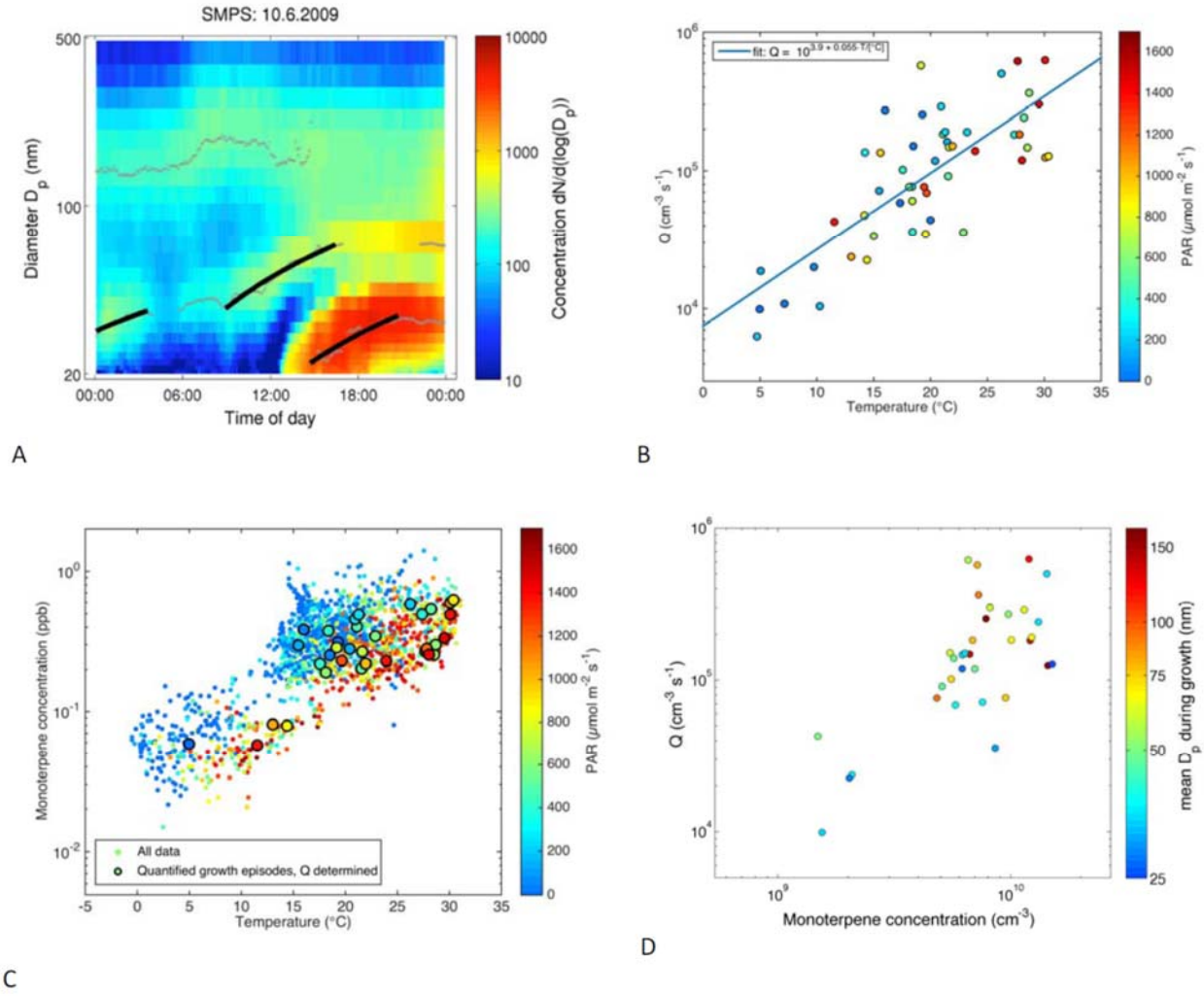

Figure 2: Particle growth rates obtained from particle number size distribution (panel A, example from day 10.6.2009). The colours indicate the measured concentrations (d*N*/d log*Dp*, cm^{-3}) of particles with different diameters (D_p, nm) over the course of a day, small circles are mean diameters of concentration modes fitted for each measurement, and the temporal change of these diameters is represented with black lines from which the growth rate is calculated. Panel B shows the calculated volumetric source rates of condensing vapours (Q, molecules cm^{-3} s^{-1}; 10-minute resolution) as a function of air temperature (°C) for all identified growth periods (one data point is obtained for each fitted growth rate, e.g. from panel A three data points would have been extracted); data are separated by levels of photosynthetically active radiation (PAR). Panel C: Monoterpene concentrations (half hourly data) measured above the canopy *vs.* temperature measured at the same level (data separated by PAR, the data points overlapping with determined growth rate in panel B are indicated by encircled symbols). ~~(data separated by PAR, the data applied in panels B and D are indicated by encircled symbols)~~, and relationship between volumetric source rate of condensing vapours and monoterpene concentration (D; data separated by particle diameter). Data points in panel (D) correspond directly to encircled symbols in panel B.

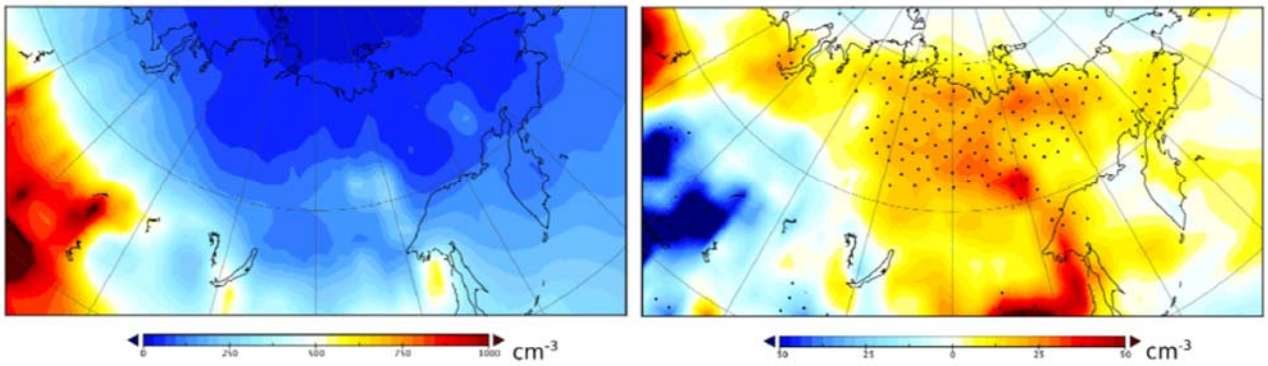

Figure 3. Annual average boundary-layer CCN (1.0%) concentration (cm^{-3}) in Siberia with present-day anthropogenic and BVOC (for BNS: E*=1.9) emissions (left panel), and changes in CCN (1.0%; right panel) concentration due to increase in BVOC emission between years 2000 and 2100 (simulations with CO_2 inhibition off). Areas with statistical significant changes in CCN are indicated by dots. The statistical analysis is based on monthly average CCN concentrations from 5-years of simulated data, and statistical significance of the CCN anomaly is evaluated using a two-sample t test, without assuming equal variance between the two populations.

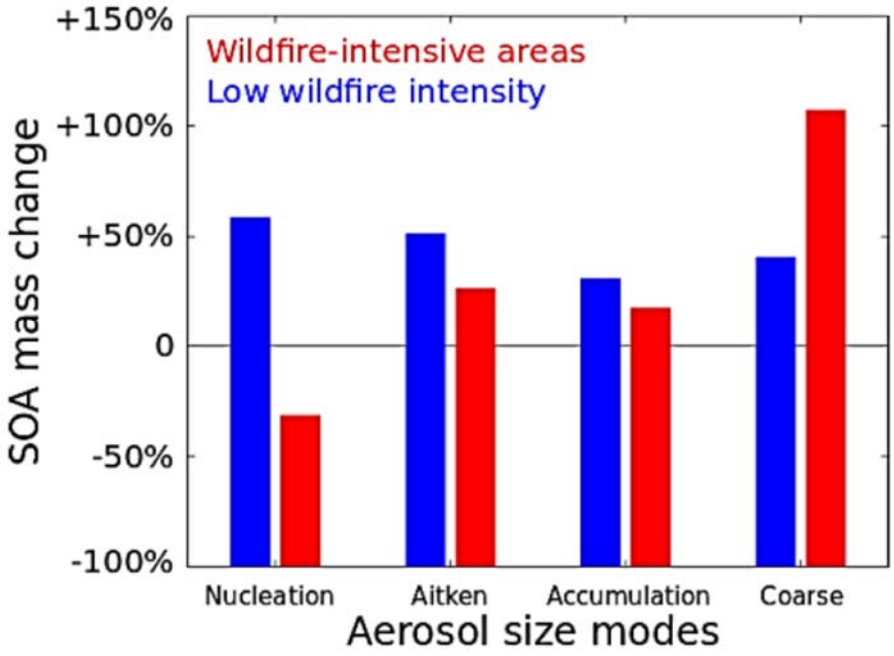

Figure 4. Relative increase in SOA mass, simulated by ECHAM5-HAM in different aerosol size modes due to BVOC emissions increase from the year 2000 to 2100. The areas are averaged over Siberia, and the BVOC emissions for years 2000 to 2100 (example is for = E^* 1.9). Areas were separated by wildfire emissions (using an emission limit of 10^{-11} kg m^{-2} s^{-1}). In the Siberian domain, accumulation mode includes over 85% of organic aerosol, and the absolute changes in SOA are also dominated by accumulation mode. However, the SOA condensation increase until year 2100 is essential for nucleation and Aitken mode growth.

Appendix:

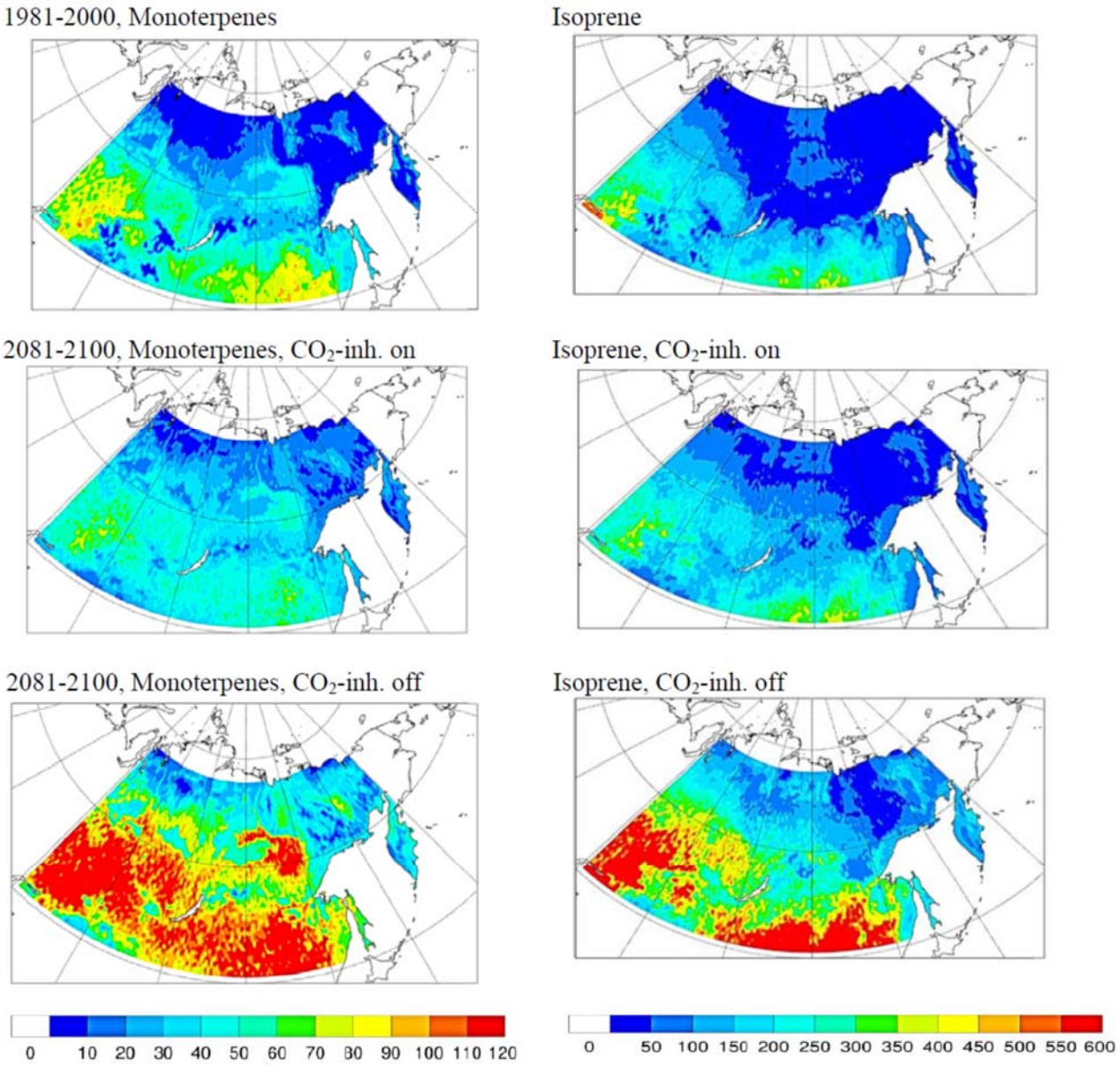

Figure A1: Present-day (top: 1981-2000) and end of 21st century (bottom: 2081-2100) total monoterpene (left) and isoprene (right) emissions for the month July ($mg_C\ m^{-2}\ month^{-1}$). Future ~~Simulations~~ simulations show results with CO_2 inhibition switched on and off; for present-day conditions the CO_2-effect on BVOC is marginal as the values are close to the standardised concentration of 370ppm, and therefore only the patterns without CO_2-effect is shown.

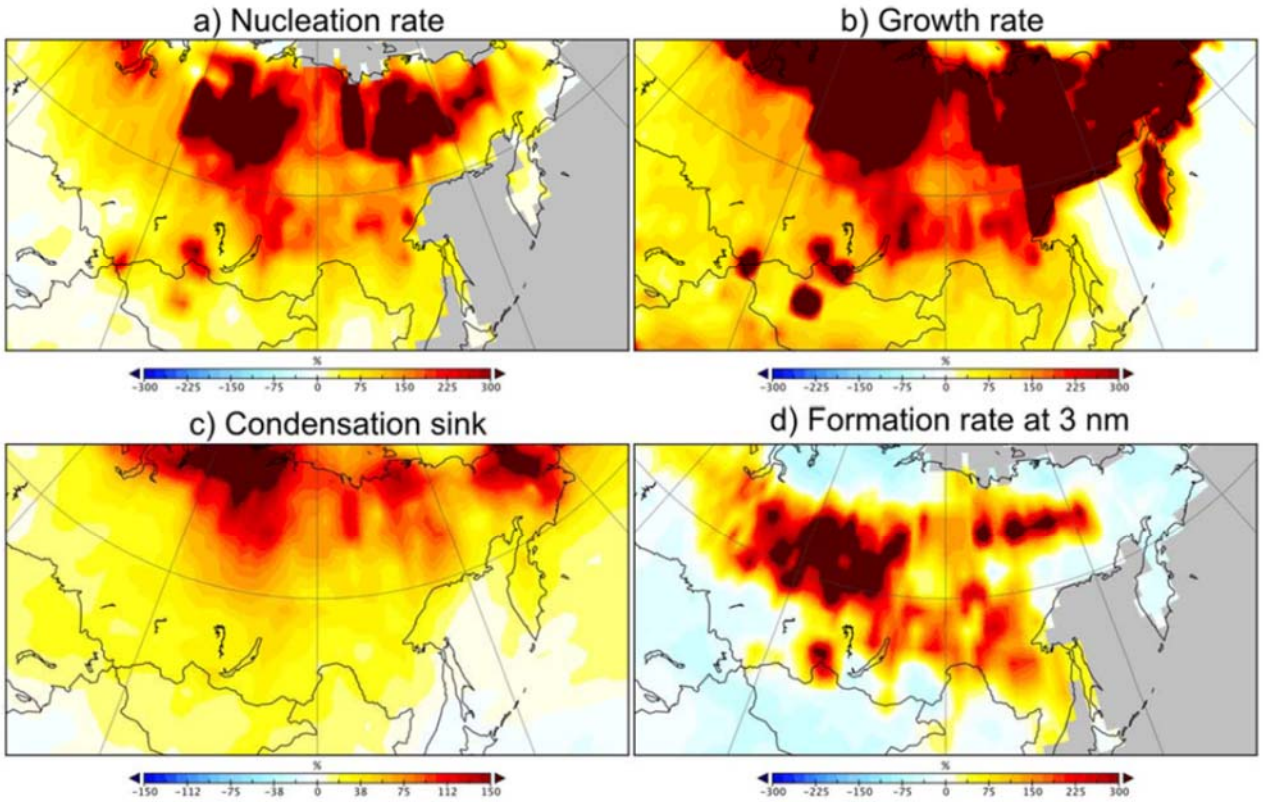

Figure A2: Relative change between years 2000 and 2100 (%) nucleation rate (a), growth rate (b), condensation sink (c) and formation rate of 3 nm particles in response to altered BVOC emissions (see methods).

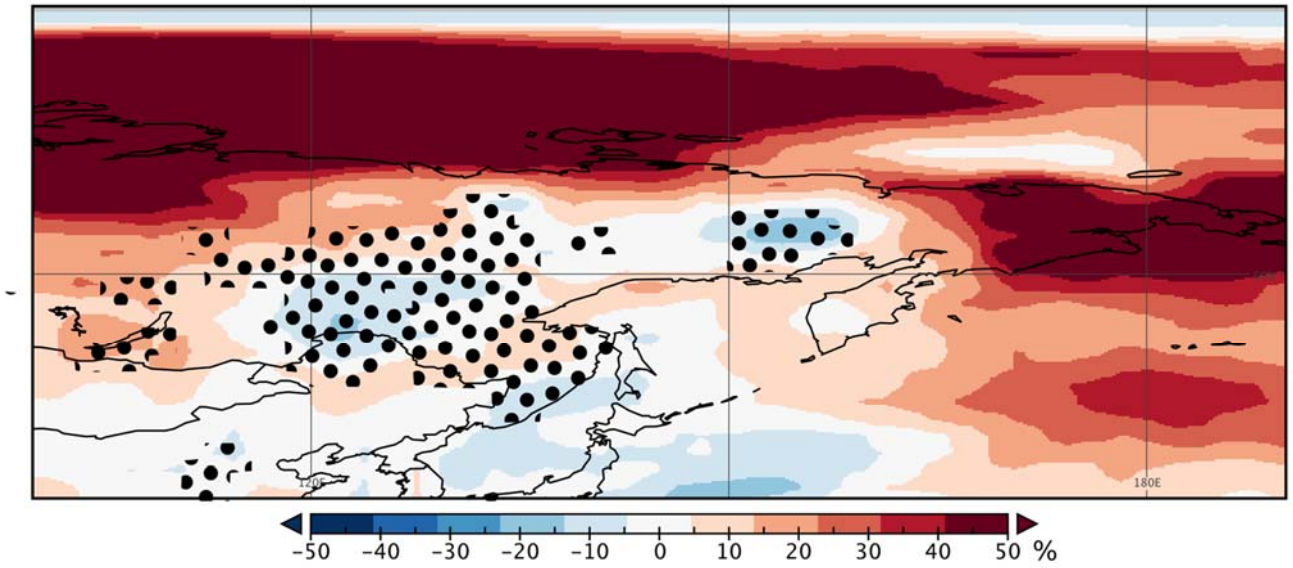

Figure A3: Relative change in summer average (June-July-August, averaged over five years) CCN(0.2%) concentration in response to altered BVOC emissions (see methods). Dotted areas denote regions where summer wildfire emission exceeds 10^{-11} kg m^{-2} s^{-1} (see Figure 4).